2023 DRAFT COASTAL MASTER PLAN

RISK ASSESSMENT MODEL IMPROVEMENTS

ATTACHMENT E2

REPORT: VERSION 01
DATE: MARCH 2021
PREPARED BY: JORDAN R. FISCHBACH, DAVID R. JOHNSON, MICHAEL T. WILSON, NATHAN B. GELDNER, CHUCK STELZNER

COASTAL PROTECTION AND
RESTORATION AUTHORITY
150 TERRACE AVENUE
BATON ROUGE, LA 70802
WWW.COASTAL.LA.GOV

COASTAL PROTECTION AND RESTORATION AUTHORITY

This document was developed in support of the 2023 Coastal Master Plan being prepared by the Coastal Protection and Restoration Authority (CPRA). CPRA was established by the Louisiana Legislature in response to Hurricanes Katrina and Rita through Act 8 of the First Extraordinary Session of 2005. Act 8 of the First Extraordinary Session of 2005 expanded the membership, duties, and responsibilities of CPRA and charged the new authority to develop and implement a comprehensive coastal protection plan, consisting of a master plan (revised every six years) and annual plans. CPRA's mandate is to develop, implement, and enforce a comprehensive coastal protection and restoration master plan.

CITATION

Fischbach, J.R., Johnson, D.R., Wilson, M.T., Geldner, N.B., Stelzner, C. (2021). 2023 Draft Coastal Master Plan: Risk Assessment Model Improvements. Version I. (pp. 1-78). Baton Rouge, Louisiana: Coastal Protection and Restoration Authority.

ACKNOWLEDGEMENTS

This document was developed as part of a broader Model Improvement Plan in support of the 2023 Coastal Master Plan under the guidance of the Modeling Decision Team (MDT):

- Coastal Protection and Restoration Authority (CPRA) of Louisiana – Elizabeth Jarrell, Stuart Brown, Ashley Cobb, Catherine Fitzpatrick, Krista Jankowski, David Lindquist, Sam Martin, and Eric White
- University of New Orleans – Denise Reed

This document was prepared by the 2023 Coastal Master Plan Risk Assessment Team:

- Jordan Fischbach – RAND Corporation
- David Johnson – Purdue University
- Michael Wilson – RAND Corporation
- Nathan Geldner – Purdue University
- Chuck Stelzner – RAND Corporation

We are grateful for the constructive reviews of this document from our colleagues Lance Menthe (RAND) and Ed Link (Maryland). Colleagues from The Water Institute including Hugh Roberts, Scott Hemmerling, Brett McMann, and Zach Cobell contributed insights to this effort. We thank Mikaela Meyer (Carnegie Mellon University) for supporting structure inventory development and other model improvements as a RAND Summer Associate. David DeSmet (RAND) assisted with final document preparation.

EXECUTIVE SUMMARY

The Coastal Louisiana Risk Assessment (CLARA) model was originally created by researchers at RAND Corporation to support development of Louisiana's 2012 Coastal Master Plan. It is designed to estimate flood depth exceedances, direct economic damage exceedances, and expected annual damage in the Louisiana coastal zone. The model uses high-resolution hydrodynamic simulations of storm surge and waves as inputs. Monte Carlo simulation is used to estimate risk under a range of assumptions about future environmental and economic conditions and with different combinations of structural and nonstructural risk reduction projects on the landscape.

This report describes a series of improvements made to the CLARA model in support of Louisiana's 2023 Coastal Master Plan, resulting in a third major version of CLARA (CLARA v3.0). The process of model improvement is similar to that conducted in support of the 2017 Coastal Master Plan. However, the model updates are more modest in scope than those implemented for the previous plan, reflecting a relatively stable approach for coastal flood risk and damage assessment and a relatively mature stage of model development. Key improvements described here were identified through an initial phase of investigation by the Risk Assessment Team, in consultation with CPRA and its Predictive Model Technical Advisory Committee (PM-TAC).

Key changes described in this report include:

- Updates to the CLARA model grid, unit of analysis, and mapping capabilities
- Creation of a novel data set comprising the location and risk-relevant attributes for structures in the coastal zone
- Implementation of advancements to joint probability modeling methodologies developed by the US Army Corps of Engineers
- Selection of a new reduced storm set for use in flood risk estimation
- Development of a new population growth scenario
- Incorporation of uncertainty in population change and structural attributes into the model's parametric uncertainty framework
- Addition of risk metrics that summarize expected direct economic losses over time
- More realistic fragility modeling that accounts for the possibility of levee failures to occur during surge runup

Some aspects of model improvements are still ongoing and expected to continue through initial testing of the 2023 Coastal Master Plan's existing conditions landscape. This report will be revised and updated to reflect the final changes used in model production.

TABLE OF CONTENTS

COASTAL PROTECTION AND RESTORATION AUTHORITY 2
CITATION 2
ACKNOWLEDGEMENTS 3
EXECUTIVE SUMMARY 4
TABLE OF CONTENTS 5
LIST OF TABLES 7
LIST OF FIGURES 7
LIST OF ABBREVIATIONS 9
1.0 INTRODUCTION 11
1.1 The CLARA Model 11
1.2 Purpose of this Report 11
1.3 Overview of Model Improvement Activities 12
1.4 Organization of this Report 12
2.0 GEOSPATIAL UPDATES 13
2.1 Updates to the CLARA Model Domain and Grid 13
Approach/Methods 13
2.2 Updating Flood Elevation Calculations 17
Analysis of Intra-Polygon Variability in Topographic Elevation 18
Usage of Grid Cell Elevations for Mapping and Risk Estimation 22
3.0 ASSET INVENTORY UPDATES 23
3.1 Structure-Level Inventory Data Sources 23
Structure Data Derived from Google Street View Imagery 26
Comparison of Microsoft/Google Data to Other Structure-Level Sources 28
3.2 Parcel-Level Asset Data Sources 30
USACE National Structure Inventory 32
CoreLogic 36
ATTOM Data Solutions 37
CoreLogic and ATTOM Summary Comparison 40
3.3 Merging Structure- with Parcel-Level Data 41
3.4 Crosswalks and Corrections for Depth Damage Curves 44

3.5 Critical Infrastructure Asset Inventory Updates 47
3.6 Structure Level Damage Analysis in CLARA 48
4.0 UPDATES TO STATISTICAL METHODS 49
4.1 JPM-OS Updates 49
4.2 Storm Selection for the 2023 Coastal Master Plan 51
4.3 Preliminary Analysis Results and Comparison 52
4.4 Final Reduced Storm Set and Analysis Results 57
5.0 ASSET GROWTH MODEL 63
5.1 Introduction 63
5.2 Approaches and Methods 63
Population Change 63
Population Response to Sea Level Rise 64
Compatibility of Hauer's Methodology with 2017 Coastal Master Plan Methodology 65
Review of Scientific Knowledge of Risk-Induced Development and Migration 65
Translating Population Growth to Assets 67
Conclusion 67
6.0 ADDITIONAL MODEL UPDATES 68
6.1 Updated or Additional Risk Metrics 68
Spatial Aggregation 68
Temporal Aggregation 69
New Damage Metrics 70
6.2 Improvements made since the 2017 Coastal Master Plan Process 70
Modeling Levee/Floodwall Fragility 70
Rainfall Model Update 71
Cross-Landscape Interpolation 71
7.0 CONCLUSION 73
8.0 REFERENCES 74

LIST OF TABLES

Table 1. Standard deviations of topographic elevations of CLARA grid polygons (meters) 19
Table 2. Comparison of Selected Structure Data Types by Source 25
Table 3. Comparison of Selected Parcel-Level Data Types by Source..... 30
Table 4. Comparison of Relative Potential Value of Dataset Contributions to CLARA 31
Table 5. ATTOM reported geocoding unavailability percentages greater than approximately 2% 38
Table 6. Data Score by Parish 43
Table 7. Summary of Asset Level Inventory by Use 46
Table 8. Root mean squared error (ft) over all sample points of the ERDC 90-storm set, relative to the 645-storm baseline..... 54
Table 9. Root mean squared error (ft) over all sample points of the final 90-storm set, relative to the 645-storm baseline..... 57
Table 10. Root mean squared error (ft) over all unenclosed points of the final 90-storm set, relative to the 645-storm baseline 59

LIST OF FIGURES

Figure 1. Splitting of 2017 Coastal Master Plan census blocks. 14
Figure 2. Splitting polygons containing multiple grid points into Thiessen polygons. 15
Figure 3. Weir void buffer effects - before corrections. 16
Figure 4. Weir void buffer effects - after corrections. 16
Figure 5. Final 2023 CLARA domain. 17
Figure 6. Visual comparison of satellite imagery to DEM skewed by major roads. ... 20
Figure 7. Map of 2023 Coastal Master Plan communities depicting the number of polygons per community with intra-polygon elevation standard deviations in excess of 2 m. 21
Figure 8. Bias in estimates of damage exceedances resulting from using grid cell polygon-averaged values for foundation heights and square footage, by return period (current conditions 2015 landscape). 28
Figure 9. Microsoft (red points) and Open Street Map (blue points) Structure Centroid Data near New Orleans displayed on CLARA model grid. 29
Figure 10. NSI coverage in Louisiana by data source. 33
Figure 11. NSI coverage: Greater New Orleans/St. Bernard example. 34
Figure 12. USACE National Structure Inventory matching methodologies near the confluence of Mississippi River and Industrial Canal. 35

Figure 13. Plaquemines Parish parcels categorized by ATTOM property descriptions and building areas (both residential and non-residential)..... 39
Figure 14. Comparison of CoreLogic and ATTOM data in the Grande Terre Estates subdivision of Belle Chase, Plaquemines Parish. 40
Figure 15. Data quality across the model domain. 43
Figure 16. Map of asset level inventory by use type for Greater New Orleans. 46
Figure 17. Synthetic storm tracks represented in the ERDC 645-storm suite. 51
Figure 18. Sample points used to evaluate reduced storm subsets. 52
Figure 19. Differences in flood depths by return period between 645- (2023) and 446-storm (2017) sets. 55
Figure 20. Differences in flood depths by return period between 645- and ERDC 90-storm sets. 56
Figure 21. Differences in flood depths by return period between the 645-storm set and the final 90-storm set. 58
Figure 22. Surge depth exceedances associated with the final 90-storm set. 60
Figure 23. Difference in surge depth exceedances between the final 90-storm set and the 2017 Coastal Master Plan's current conditions case. 61
Figure 24. Difference in surge depth exceedances between the final 90-storm set and the full 645-storm suite. 62

LIST OF ABBREVIATIONS

ACQ ..... CENTER OF THE STRUCTURE
ADCIRC ..... ADVANCED CIRCULATION
AEP ..... ANNUAL EXCEEDANCE PROBABILITY
AI ..... ARTIFICIAL INTELLIGENCE
ARIMA ..... AUTO REGRESSIVE INTEGRATED MOVING AVERAGE
ATTOM ..... ATTOM DATA SOLUTIONS
CEN ..... CENTROID OF THE PARCEL
CISA ..... CYBERSECURITY AND INFRASTRUCTURE SECURITY AGENCY
CLARA ..... COASTAL LOUISIANA RISK ASSESSMENT
CPRA ..... COASTAL PROTECTION AND RESTORATION AUTHORITY
DAAS ..... DATA-AS-A-SERVICE
DEM ..... DIGITAL ELEVATION MODEL
DHS ..... DEPARTMENT OF HOMELAND SECURITY
EAD ..... EXPECTED ANNUAL DAMAGE
ERDC ..... ENGINEER RESEARCH AND DEVELOPMENT CENTER
FEMA ..... FEDERAL EMERGENCY MANAGEMENT AGENCY
FOUO ..... FOR OFFICIAL USE ONLY
GBS ..... GENERAL BUILDING STOCK
GIS ..... GEOGRAPHIC INFORMATION SYSTEM
GOHSEP .. GOVERNOR'S OFFICE OF HOMELAND SECURITY AND EMERGENCY PREPAR-EDNESS
GSV ..... GOOGLE STREET VIEW
HAZUS-MH ..... HAZARDS U.S. MULTI-HAZARD
HIFLD ..... HOMELAND INFRASTRUCTURE FOUNDATION-LEVEL DATA
HSIP ..... HOMELAND SECURITY INFRASTRUCTURE PROGRAM
HURDAT ..... NORTH ATLANTIC HURRICANE DATABASE
ICM ..... INTEGRATED COMPARTMENT MODEL
IPCC ..... INTERGOVERNMENTAL PANEL ON CLIMATE CHANGE
JPM-OS ..... JOINT PROBABILITY METHOD WITH OPTIMAL SAMPLING
ML ..... MACHINE LEARNING

NAICS..... NORTH AMERICAN INDUSTRY CLASSIFICATION SYSTEM
NFIP ..... NATIONAL FLOOD INSURANCE PROGRAM
NGA ..... NATIONAL GEOSPATIAL AGENCY
NOAA .....NATIONAL OCEANIC AND ATMOSPHERIC ADMINISTRATION
NSI ..... NATIONAL STRUCTURE INVENTORY
OSM ..... OPEN STREET MAPS
PDD.....PRESIDENTIAL DISASTER DECLARATION
PII.....PERSONALLY IDENTIFIABLE INFORMATION
PM-TAC..... PREDICTIVE MODEL TECHNICAL ADVISORY COMMITTEE
QA/QC .....QUALITY ASSURANCE/QUALITY CONTROL
RMSE.....ROOT MEAN SQUARED ERROR
SF ..... SQUARE FOOTAGE
SLTT.....STATE, LOCAL, AND TRIBAL TERRITORIES
SSP .....SHARED SOCIOECONOMIC PATHWAYS
SWAN .....SIMULATING WAVES NEARSHORE
TIGER... TOPOLOGICALLY INTEGRATED GEOGRAPHIC ENCODING AND REFERENCING
USACE .....U.S. ARMY CORPS OF ENGINEERS
VA..... VETERANS AFFAIRS

1.0 INTRODUCTION

1.1 THE CLARA MODEL

The Coastal Louisiana Risk Assessment (CLARA) model was originally created by researchers at RAND Corporation to support development of Louisiana's 2012 Coastal Master Plan. It is designed to estimate flood depth exceedances, direct economic damage exceedances, and expected annual damage in the Louisiana coastal zone. The model uses high-resolution hydrodynamic simulations of storm surge and waves as inputs. Monte Carlo simulation is used to estimate risk under a range of assumptions about future environmental and economic conditions and with different combinations of structural and nonstructural risk reduction projects on the landscape.

The CLARA model is already well described in prior peer-reviewed and published literature, so this report does not include detailed descriptions of the basic methodological approach and assumptions. For interested readers, an introduction to the model can be found in Fischbach et al. (2012) and Johnson et al. (2013). Model improvements for the 2017 Coastal Master Plan are described in Fischbach et al. (2017), and published examples of CLARA model results can be found in Fischbach et al. (2019), Meyer and Johnson (2019), and Fischbach et al. (2017b). An updated, standalone summary of the CLARA model methodology to serve as an introduction and overview of the model is expected for publication in 2021 and will be updated for final publication with the 2023 Coastal Master Plan.

1.2 PURPOSE OF THIS REPORT

This report describes a series of improvements made to the CLARA model in support of Louisiana's 2023 Coastal Master Plan, resulting in a third major version of CLARA (CLARA v3.0). The process of model improvement is similar to that conducted in support of the 2017 Coastal Master Plan (Fischbach et al., 2017). However, the model updates are more modest in scope than those implemented for the previous plan, reflecting a relatively stable approach for coastal flood risk and damage assessment and a relatively mature stage of model development. Key improvements described here were identified through an initial phase of investigation by the Risk Assessment Team, in consultation with CPRA and its Predictive Model Technical Advisory Committee (PM-TAC).

This report should be of interest to CPRA and technical professionals and researchers in the field of flood risk assessment. This report version reflects data upgrades and model improvements made as of December 2020. Given current progress on model simulation, further updates will be needed in

order to fully document model changes related to future scenario evaluation and nonstructural project assessment. As a result, at least one update to this report is anticipated in early- to mid-2021 once these approaches are finalized.

1.3 OVERVIEW OF MODEL IMPROVEMENT ACTIVITIES

For the 2023 Coastal Master Plan, key improvements and changes include (1) updates to CLARA's geospatial domain and grid, with the goal of correcting minor issues identified during the 2017 Coastal Master Plan analysis; (2) updates to the statistical methodology for estimating flood likelihood, including a new experimental design of simulated storms; (3) updated methods for considering future population and asset growth; (4) a broader range of damage outputs; and (5) other minor improvements to the model's handling of system fragility and risk estimates in time periods not run through ADCIRC+SWAN.

Of particular note in this update is a new inventory of assets in the coastal zone derived from newly available parcel- and structure-level datasets, with specific structure locations, first-floor elevation estimates, and other key details now included for each structure. CLARA v3.0 uses structures as the unit of analysis for damage calculations, although risk estimates are still aggregated to larger spatial units for communication purposes. This report describes in detail the methods for both building this new structure-level dataset and incorporating it into the CLARA damage model, respectively.

1.4 ORGANIZATION OF THIS REPORT

This report is organized into seven chapters. Chapter 2 describes updates to CLARA's geospatial grid, the unit of resolution used to estimate flood depth for each location across the coast. The new structure-level dataset and implementation in the CLARA damage model is described in Chapter 3. Chapter 4 documents revised statistical methods for estimating flood depths and the process for selecting a new set of simulated storms for the quantitative experiments. Chapter 5 focuses on new population growth projections for future damage analysis, while Chapter 6 provides an overview of the revised damage metrics. The report concludes with a brief summary of key advances in Chapter 7.

2.0 GEOSPATIAL UPDATES

2.1 UPDATES TO THE CLARA MODEL DOMAIN AND GRID

Previous versions of the CLARA model have utilized a study domain designed to encompass the estimated 2,000-year floodplain 50 years in the future. In 2017, the domain also included Mississippi's three coastal counties, for the purpose of evaluating potential impacts of a Lake Pontchartrain barrier; it also included a portion of coastal Texas, but due to a lack of quality topographic elevation and economic asset data, points in Texas were ultimately excluded from the 2017 analysis.

The model grid in 2017 consisted of grid points paired to polygons. The spatial unit of analysis was based on a regularly-spaced 1 km grid,[1] with additional points placed in areas with relatively high population density, such that every 2010 U.S. census block would contain at least one CLARA grid point. In smaller blocks, the grid point was placed at the block's centroid (instead located at a representative central location if the centroid lay outside the block boundary). In larger blocks, grid points defaulted to the regularly spaced grid.

Mapped visuals were generated using grid cell polygons formed by Thiessen polygons enclosing each of the grid points, such that a given point's polygon consisted of all spatial locations closer to that grid point than any other. This meant that grid cell polygons did not necessarily conform to census or municipal boundaries. Further, some grid cell polygons also crossed water features and levee/floodwall centerlines. Consequently, flood maps produced using CLARA outputs could convey misleading information about risk near protection features, or they could otherwise appear unnecessarily jagged due to the use of Thiessen polygons. CLARA v3.0 corrects for these issues in order to improve the communication of flood risk results in the 2023 Coastal Master Plan.

APPROACH/METHODS

The starting point for the grid update is the set of 2010 U.S. census blocks (98,514 GIS polygons) which made up the 2017 Coastal Master Plan model domain. These census blocks were split by the boundaries of municipalities and incorporated places defined by the 2019 Census TIGER line files (U.S. Census Bureau, 2019), yielding 100,552 polygons. Then, an overall line dataset was created

[1] Due to the curvature of the earth's surface, there is small variance (<5 m) in the nominally 1 km spacing between a given regularly spaced point and the regularly spaced point to the north or south of it.

from several constituent datasets:

- Project lines of Structure Type “Levee” (CPRA, May 2019)
- Levee alignments generated for a Sea Grant project (Louisiana State University (LSU) Agricultural Center, June 2016)
- Levee alignments used in ADvanced CIRCulation (ADCIRC) model (USACE, April 2019)
- The final hurricane protection system lines from the 2017 Coastal Master Plan (CPRA, March 2017).

This overall project line dataset was then used to further split the polygons, yielding 118,719 polygons (Figure 1).

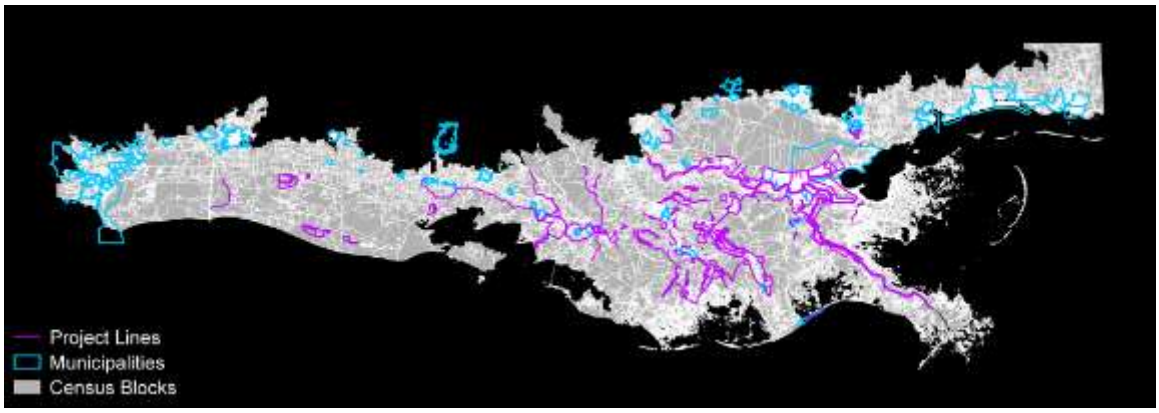

Figure 1. Splitting of 2017 Coastal Master Plan census blocks.

These split polygons were then compared to the 113,692 model grid points used in the 2017 Coastal Master Plan. Each polygon containing zero grid points was assigned a newly created grid point located at the polygon’s center. As shown in Figure 2, each polygon containing multiple grid points was split into one polygon per contained grid point, such that the resulting set of Thiessen polygons each represented the area closest to its single grid point. Each polygon containing exactly one grid point was left as is. This further polygon splitting resulted in 134,590 polygons (referred to below as grid polygons), and the same number of grid points.

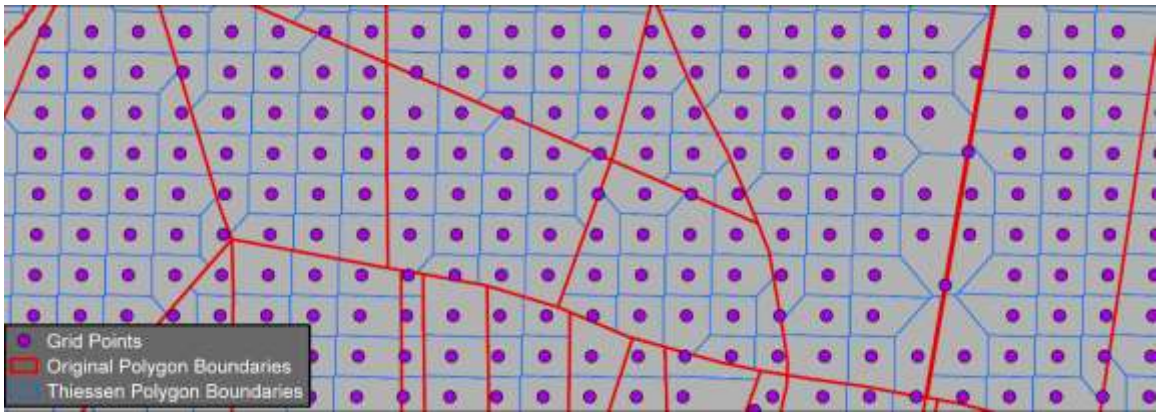

Figure 2. Splitting polygons containing multiple grid points into Thiessen polygons.
Though grid points may appear to lie on a resulting polygon boundary, the points are simply very close to a boundary and do not intersect it. Note also that the resulting set of polygons is a merging of the original and Thiessen polygon boundaries. As such, the Thiessen Polygon Boundaries as shown also exist directly underneath each of the Original Polygon Boundaries.

At this point, the team considered polygons representing ADCIRC weir voids: areas where ADCIRC model data would not be available, and inside which grid points should not be placed. The weir void polygons were buffered by 5 m to allow for geolocational error, and the weir buffer was overlaid with the original census blocks, the grid polygons, and the grid points to determine overlap. The spatial relationships of interest are:

- Grid polygons within census blocks which themselves fall entirely inside the weir buffer.
- Aside from the bullet above, grid polygons which fall entirely inside the weir buffer.
- Other than polygons in the bullets above, grid cell polygons which fall partially inside the weir buffer.

An example of these is shown in Figure 3.

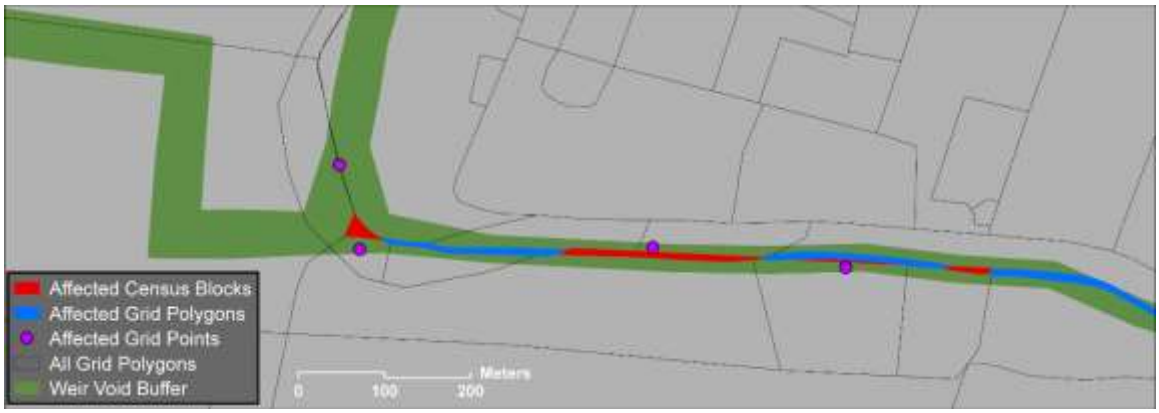

Figure 3. Weir void buffer effects - before corrections.

Polygons falling entirely inside a weir buffer, which belong to a census block which was not itself entirely contained within the weir buffer, were merged together on the ID of their parent census block.

Then this set of polygons, and grid polygons within census blocks entirely within the weir buffer, were combined. Each polygon in the combined set was merged with exactly one neighboring grid polygon which did not fall entirely inside the weir buffer. A table is used to note the ancestry of each of the polygons combined in this way, which will be used to enable proportional distribution of population and housing data to the new, combined polygons.

Finally, other grid polygons which fell inside the weir buffer only partially were considered. If their grid points fell inside the weir buffer, then those grid points were each snapped to (relocated to coincide with) the nearest location along the weir buffer boundaries.

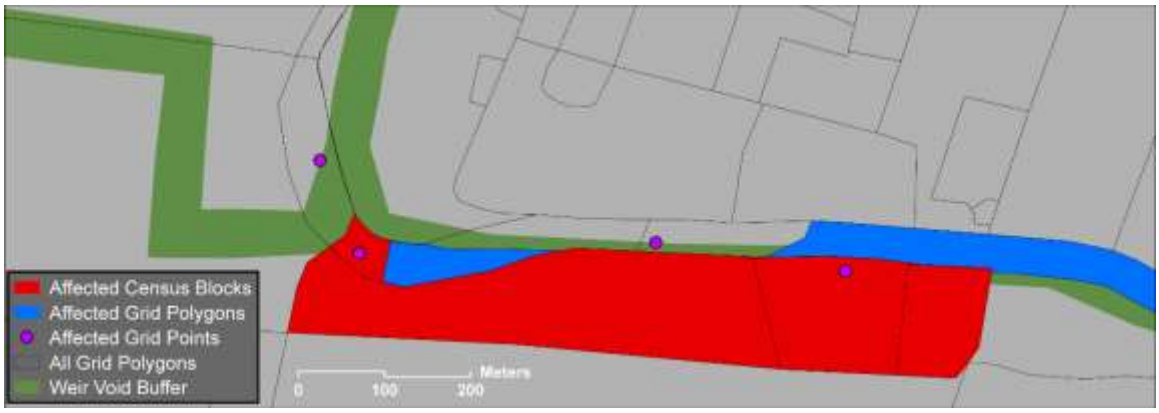

Figure 4. Weir void buffer effects - after corrections.

This procedure – splitting and reconciliation with weir void polygons – was applied with respect to the final project lines, with additional splitting along Integrated Compartment Model (ICM) compartment and additional community boundaries. This yielded a CLARA mesh consisting of 126,174 grid points, contained within the final domain shown in Figure 5 below.

Figure 5. Final 2023 CLARA domain.

2.2 UPDATING FLOOD ELEVATION CALCULATIONS

In previous versions of the CLARA model, the spatial unit of analysis consisted of paired grid cells and points. Grid cells are represented by polygons, while grid points are primarily located at the centroid of the corresponding grid cell polygon. Surge and wave characteristics were extracted from the ADCIRC and Simulating WAves Nearshore (SWAN) models at the grid point locations, and it was assumed that those values were representative of the surge and wave behavior at all points within the grid cell polygon. Further, the topographic/bathymetric elevation of the grid point was used when converting surge elevations and wave heights to peak flood depths.

In a small number of instances, grid points were located in channels, culverts, or other narrow low-elevation features within a grid cell polygon that was otherwise predominantly land. This resulted in the grid point being assigned an elevation value that was not representative of the elevation of inhabited land in its grid cell polygon, resulting in the possibility of flood depths being biased upwards for large portions of the grid cell polygon. This effect showed up in flood maps as polygons with substantially higher flood depth exceedances than neighboring polygons, and it may have biased damage calculations for assets within those grid cell polygons.

To safeguard against this issue occurring in the 2023 Coastal Master Plan, two changes were made to the treatment of topographic elevations. Firstly, the team ensured that the grid point locations where

ADCIRC/SWAN data are extracted are not located in engineered low-elevation features, such as dredged channels or culverts that can be identified in the current conditions digital elevation model (DEM). This was done similarly to the process applied to manually move grid points that were located in weir voids in the ADCIRC mesh during the 2017 Coastal Master Plan. Secondly, the elevation used to calculate flood depths for any grid cell polygons containing land is no longer simply the topographic or bathymetric elevation at the grid point's location. Instead, the team assigned an elevation equal to the areal median topographic elevation from the digital elevation model (DEM) over all land pixels within the grid cell polygon, as determined by the land-cover raster for each current or future landscape.

ANALYSIS OF INTRA-POLYGON VARIABILITY IN TOPOGRAPHIC ELEVATION

To support this decision, the team assessed the degree to which the median and mean elevation of land pixels are representative of topographic elevations within each grid cell polygon. While risk calculations will be based upon topographic elevations at the precise point where assets are located, the analysis supports the notions that (i) an areally-averaged topographic elevation is broadly representative of all points within a single grid cell polygon, and (ii) peak water surface elevations from individual storms should have low variation within grid cell polygons, based on topographic considerations. Ultimately, the team decided to apply the areal median in each grid cell instead of the mean because of its robustness to outlier pixels.

Table 1 shows the number and percentage of CLARA grid polygons in Louisiana and Mississippi with a particular range of variability in topographic elevation, as characterized by the standard deviation in meters. The large majority of polygons are fairly uniform in their topographic elevation, with 80% having standard deviations less than 0.5 m, and 92% having standard deviations less than 1 m.

Table 1. Standard deviations of topographic elevations of CLARA grid polygons (meters)

Elevation Standard Deviation (m)	Polygon Count	Percent of Polygons
0.0 - 0.5	104,325	80.3
0.5 - 1.0	15,760	12.1
1.0 - 1.5	4,416	3.4
1.5 - 2.0	2,120	1.6
2.0 - 2.5	968	0.7
2.5 - 3.0	562	0.4
3.0 or greater	1821	1.4

We visually inspected some of the polygons with outlier standard deviations, and grid cell polygons with large differences in their mean elevations compared to neighboring polygons, using satellite imagery. The bulk of these polygons with large variability and anomalous elevations were due to natural features such as the Avery Island and Weeks Island salt domes, while some were due to the presence of human-made structures such as elevated roadways. See Figure 6 for an example of an area where mean elevations have been skewed due to the presence of an elevated roadway.

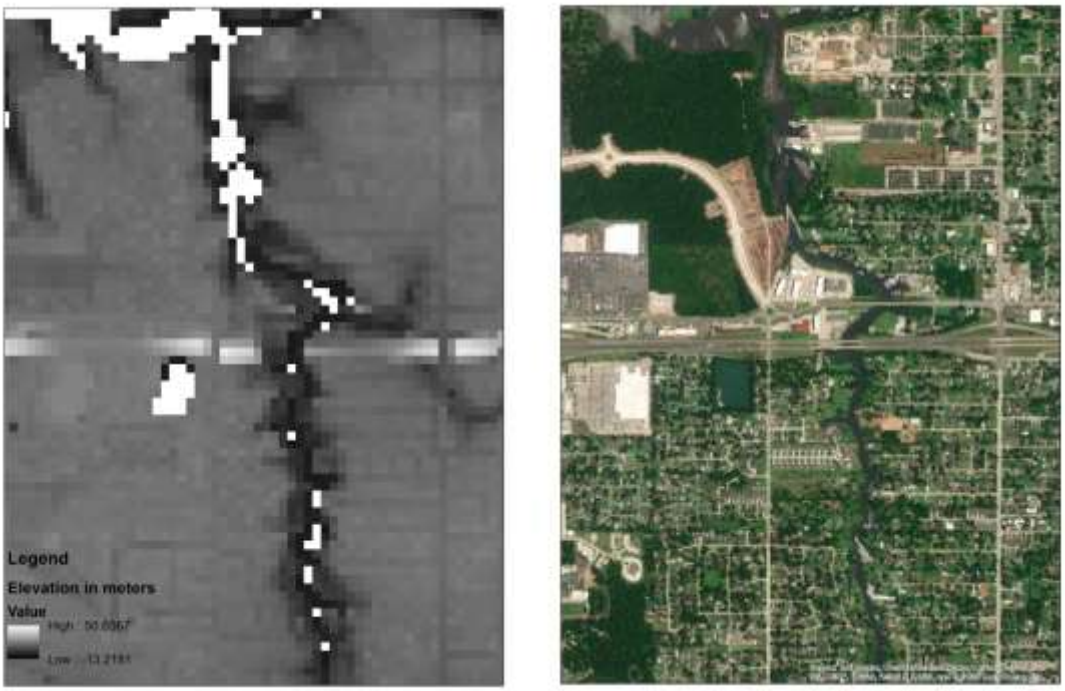

Figure 6. Visual comparison of satellite imagery to DEM skewed by major roads. Note how the elevated roadway going from east to west in the middle of the image is clearly visible in the DEM (left) as it is in the satellite image (right).

Figure 7 shows the number of polygons within each of the 2023 Coastal Master Plan communities with a standard deviation of topographic pixel elevations over 2 m (totaling roughly 2.5% of all Louisiana grid cells).[2] Communities not shown had no polygons with standard deviations over 2 m. Outlying grid cells with larger elevation variability typically occur in higher-elevation inland communities such as Lake Charles and Covington, although some parts of St. Mary Parish also have this property.

[2] The community boundaries described here were developed by a partner team at The Water Institute and will be documented in a separate appendix to the master plan.

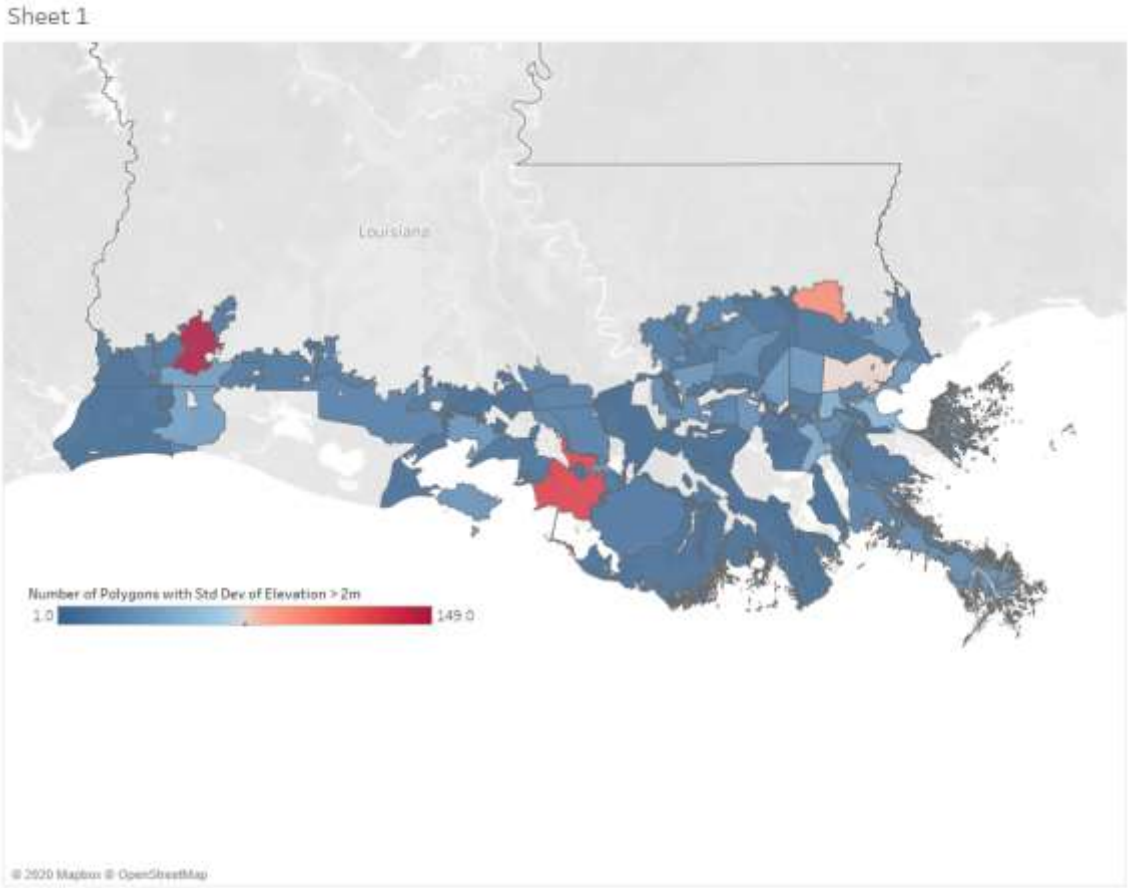

Figure 7. Map of 2023 Coastal Master Plan communities depicting the number of polygons per community with intra-polygon elevation standard deviations in excess of 2 m.
Base layer indicates community has zero such polygons.

Comparing median land elevations to the grid point elevations assigned in the 2017 Coastal Master Plan provides additional insight into data quality and improvements in flood depth mapping that can be achieved for the 2023 Coastal Master Plan: 95.4% of 2023 polygons have median elevations within 1 m of the elevation assigned to a corresponding 2017 grid point; 97.1% are within 2 m. Further, the median and mean elevations are within 0.5 m of each other for 96.7% of grid cells, and within 1 m of each other for 98.9%.

USAGE OF GRID CELL ELEVATIONS FOR MAPPING AND RISK ESTIMATION

The median elevations assigned to each grid cell polygon are used as the basis for the development of flood maps and as an input to CLARA's economic module. Each polygon has a representative point location associated with it where surge elevations will be extracted from the ADCIRC model. These surge elevations are assumed to be representative of surge throughout the polygon. The surge elevation, wave height, and median land elevation are used to generate flood depths on an individual storm basis for QA purposes, and are also used to generate storm surge and wave statistics to produce exceedance maps.

In the economic model, surge and wave exceedance information is retained at the polygon level. For structural assets, these are used to calculate flood depth exceedances at each asset's location. The topographic elevation associated with each asset, used to calculate flood depths, is taken from the DEM pixel containing the centroid of the structure's footprint. The median polygon elevation is used in the economic module for estimating risk to nonstructural assets such as agricultural crops and roads.

3.0 ASSET INVENTORY UPDATES

Since the 2017 Coastal Master Plan, there has been a substantial increase in the quality and quantity of detailed, parcel-level land use and structure-level inventory data. This section describes the investigation of various parcel-level datasets currently available for coastal Louisiana and their potential strengths and weaknesses. This includes a description of how key inputs that might be incomplete or missing from existing sources, such as first-floor elevation or number of stories, could be augmented with recently conducted analysis. The report next discusses data acquisition, aggregation, and quality assurance/quality control conducted to produce a new structure-level asset inventory to inform CLARA risk assessment. Finally, this section concludes by describing how these data map to support structure-level damage calculations.

3.1 STRUCTURE-LEVEL INVENTORY DATA SOURCES

The best available asset inventory data at the time of the 2017 Coastal Master Plan analysis was assembled from several different sources, reflective of updates at different points in time at different levels of resolution. For example, the CLARA team was able to obtain individual parcel-level data from US Army Corps of Engineers (USACE) feasibility studies for selected regions (e.g., Morganza to the Gulf; Southwest Coastal), whereas for other regions the best available data were from older post-Katrina economics studies and only available as aggregate counts without detail on structure location or other attributes (Fischbach et al., 2017).

Given limited data availability, the 2012 and 2017 Coastal Master Plans began with data aggregated by census block as a starting point for the asset inventory. This was found to be problematic when addressing lightly populated spatial units spanning relatively large areas. For the 2017 Coastal Master Plan, the project team used LandScan population estimates (Bhaduri et al., 2007) to improve the assignment of assets to specific grid cells, but the interpolation process introduced the potential for additional error or difficulty in interpreting. For example, this approach necessitated assigning fractional numbers of structures to each grid cell in lightly populated census blocks where specific asset locations were unknown.

For the 2023 Coastal Master Plan, preliminary investigations suggested that it is now possible to assemble a structure-level database for the entire coastal region based on existing data sources: Microsoft building footprints[3] blended with Google Street View[4] (MS/GSV), both generated by artificial

[3] Publicly available at: https://github.com/Microsoft/USBuildingFootprints
[4] Method described subsequently and in Chen et al. (under review).

intelligence (AI) and machine learning (ML) algorithms, USACE National Structure Inventory (NSI), and the Open Street Maps (OSM) building data layer for the State of Louisiana. Note that the NSI draws in part on Microsoft's building footprint data, as well as additional data from Esri Business Analyst, the U.S. Census, and FEMA's HAZUS-MH software. Table 2 compares the relative number of structures in the model domain and the types of associated data by source.

Table 2. Comparison of Selected Structure Data Types by Source

	MICROSOFT BUILDING FOOTPRINTS WITH GOOGLE STREET VIEW	NSI (CORELOGIC, ESRI BUSINESS, HAZUS, CENSUS)	OPEN STREET MAPS BUILDING LAYER
STRUCTURES IN MODEL DOMAIN	780,715	746,005	171,700 (SEE NOTE)
DATA TYPE	POLYGON AND POINT	POINT	POLYGON
ADDRESS	X		
BUILDING TYPE	X	X	
PROPERTY USE		X	
BUILDING AREA		X	
ASSESSED VALUE		X	
CONTENT VALUE		X	
VEHICLE VALUE		X	
YEAR BUILT (>1992)		X	
ESTIMATED STORIES		X	
ESTIMATED RESIDENTIAL UNITS		X	
BASEMENT PRESENCE		X	
CONSTRUCTION MATERIAL		X	
FOUNDATION TYPE AND ESTIMATED HEIGHT	X	X	
ESTIMATED GROUND ELEVATION	X	X	
ESTIMATED FINISHED FLOOR ELEVATION	X		
NFIP DATA		X	
CENSUS SOCIAL VULNERABILITY DATA		X	

Note: As a user-generated data source, OSM does not contain a complete inventory and has uneven coverage, typically offering more detail in more densely built areas.

Since the 2017 Coastal Master Plan, numerous local, state, and national organizations and governments have developed property-level flood analyses. For example, North Carolina's Flood

Insurance Rate Map viewer[5] or First Street Foundation's Flood Factor[6] both examine residential assets at these levels, though with potentially varying levels of specificity and resolution within a particular geographic area or type. The new CLARA asset inventory, given a wider variety of property-level uses intended for analysis, applies a structure-level approach while retaining characteristics derived from parcel-level datasets. For example, a university, oil tank farm, or offshore vessel port service area have single ownership with large land areas, but the structures located on these parcels may have substantially different exposures and vulnerabilities. In order to balance this level of detail with the need for computational efficiency across the simulation runs, and given coastal Louisiana's relatively low variation in topography, the parcel-level characteristics were applied to each structure centroid.

STRUCTURE DATA DERIVED FROM GOOGLE STREET VIEW IMAGERY

In CLARA, the key structure attributes needed to inform risk estimates are the first-floor elevation, foundation type, square footage, and structure type (e.g., residential, commercial). For residential assets, valuation also relies upon the number of stories, construction quality, and the presence of a garage. For non-residential assets, valuation is based on an assumed replacement cost per square foot associated with the given building type, defined by HAZUS General Building Stock (GBS) codes (FEMA, 2009).

As outlined in previous sections, other structure-level datasets may not contain some of these key attributes, particularly first floor elevation. However, the team has access to a coastwide dataset containing estimated structural attributes produced by applying automated image analysis to Google Street View (GSV) images. A team led by David Johnson utilized convolutional neural networks and a novel task relation encoding network to estimate first floor foundation and to classify buildings by residential or non-residential; foundation type as pier, concrete slab-on-grade, or other; and number of stories (Chen et al., under review). The learning algorithms were trained on 42,415 GSV images of properties in data from the Morganza to the Gulf Reformulation study (USACE, 2013), Southwest Coastal Louisiana Feasibility study (USACE, 2016), West Shore Lake Pontchartrain Feasibility study (USACE, 2014), and FEMA Elevation Certificates compiled by Jefferson Parish. The training data consists of structures from a total of ten coastal parishes, and the GSV imagery was acquired in 2018; the actual date of each image varies, but Google has typically refreshed GSV coverage in coastal Louisiana communities every one to four years, with more frequent updates occurring in urban areas such as New Orleans.

Seventy percent of the reference images were used to train the building detection and attribute prediction models. Ten percent were used to calculate validation loss for every epoch of the learning

[5] North Carolina's Flood Information Center available at: https://flood.nc.gov/ncflood/
[6] First Street Foundation Flood Factor available at: https://firststreet.org/flood-factor/

process, and 20% were used to validate performance of the final models. The machine learning predictions have a mean absolute error of 0.17 m for first floor elevation and prediction accuracies of 82.1% for foundation type, 93.7% for building type, and 98.3% for the number of stories. Model outputs for the three classification tasks also include confidence scores.

In parts of the CLARA model domain where structure-level information was not available for the 2017 Coastal Master Plan, CLARA previously applied average foundation heights by structure and foundation type taken from street-level surveys done by USACE in the 1990s. As such, utilizing the results from the GSV image analysis in the 2023 Coastal Master Plan will provide both a distribution of foundation heights within grid cell polygons (or structure-level first floor elevations if structure-level modeling is performed) and much more current estimates. Usage of spatial distributions of structural attributes in CLARA v3.0 is described in more detail in Section 3.6.

Figure 8 shows the bias in damage estimates introduced by using average foundation heights and square footage for approximately 40,000 structures in the machine learning training data (all training data described above except for the Jefferson Parish assets), relative to the estimates from using their ground truth values for those two structural attributes. The figure presents bias by return period under the 2017 Coastal Master Plan's current conditions landscape, where the percentage illustrated represents the proportional bias after summing up the damage estimates over all of the structures. This reveals that in the parishes where training data were available, using average values produces underestimates of risk from higher-frequency events, while overestimating risk from events with return periods greater than 50 years.

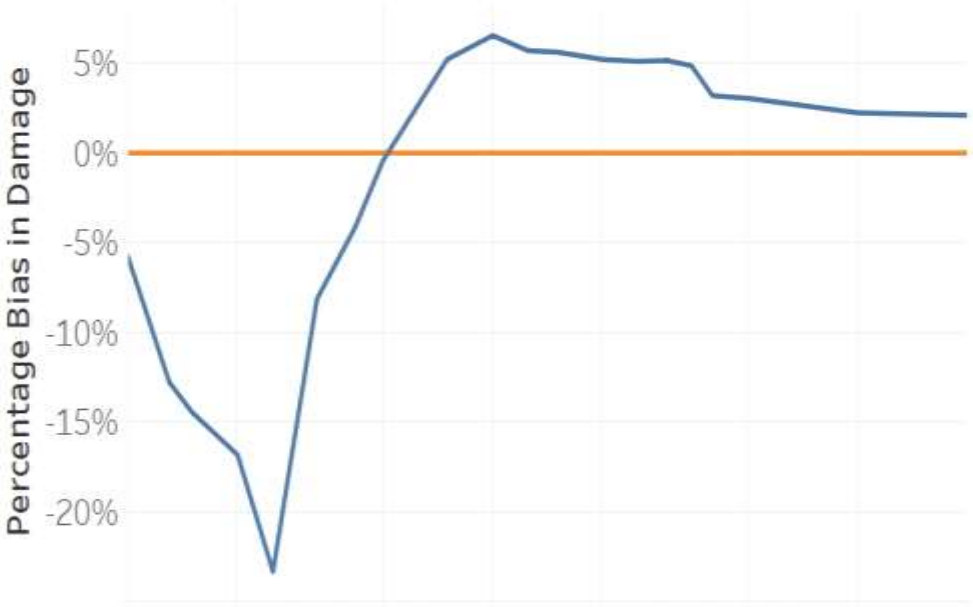

Figure 8. Bias in estimates of damage exceedances resulting from using grid cell polygon-averaged values for foundation heights and square footage, by return period (current conditions 2015 landscape).

The above analysis only represents bias from using average foundation heights and square footage; it does not account for hyperlocal estimates of topographic elevations (i.e., the difference between topographic elevations at the location of a structure and the elevation assumed for its associated CLARA grid cell polygon), or other specific structural attributes. However, this limited analysis is suggestive of the value of using structure-level attributes.

COMPARISON OF MICROSOFT/GOOGLE DATA TO OTHER STRUCTURE-LEVEL SOURCES

A comparison of Microsoft building footprint data relative to aerial imagery revealed it was more accurate and complete than either NSI or OSM.[7] As NSI also draws in part upon the Microsoft data, the MS/GSV data was selected as the primary "key" to match with other sources. In reviewing this data source, several artifacts of the AI/ML process were identified, such as tiling issues or attached structures being read as single buildings. These were particularly evident in the French Quarter and other dense areas of Orleans Parish. To improve the data quality in these areas and fill these gaps, the

[7] OSM only had coverage in selected urban areas as a user-generated, non-systematic data resource. In contrast, NSI pulled upon several foundational data sources, but in several locations was clearly out of date relative to recent (re)development or had an extensive number of centroids located in wetlands and over water where there were clearly no structures.

centroid of the OSM footprints were appended. Across the model domain, 32,319 OSM structures had a centroid greater than 15 m from that of the Microsoft building data point (approximately 29,000 of these are within Orleans Parish). These OSM structure points, however, had no additional identifying information (aside from their ground square footage calculated in ArcGIS using the Southern Louisiana State Plane), necessitating a match to additional parcel data to obtain additional structure characteristics.

Figure 9 shows in orange where OSM structure data supports the base Microsoft structure data in blue (with the model domain grid polygons as a background). There is a noticeable difference in Microsoft algorithm data quality (and OSM structure data availability) to the top left and bottom right of the image in Jefferson Parish.

Figure 9. Microsoft (red points) and Open Street Map (blue points) Structure Centroid Data near New Orleans displayed on CLARA model grid.
Note potential artifacts of missing structures in the Microsoft building footprint data extending from Irish Channel to Tulane's campus, across City Park, and back toward the French Quarter and Marigny.

3.2 PARCEL-LEVEL ASSET DATA SOURCES

In order to assign asset attributes such as property use and valuation to the structures, two nationwide parcel-level datasets were compared with coverage in the Louisiana coastal zone. Each of these draws upon parish-level tax assessor data for the residential components, supplied via either CoreLogic or ATTOM Data Solutions (ATTOM).

The Homeland Infrastructure Foundation-Level Data (HIFLD, secured and licensed through the Department of Homeland Security) also includes CoreLogic and Dun & Bradstreet's commercial data. ATTOM is a proprietary purveyor of similar datasets engaged for their potentially favorable license terms, quality statistics, and additional data cleaning. Table 3 summarizes the availability of selected CLARA data inputs by database.

Table 3. Comparison of Selected Parcel-Level Data Types by Source

	HIFLD (CoreLogic, Dun & Bradstreet)	**ATTOM**
Property Use	X	X
Building Area		X
Assessed Value	X	X
Market Value		X
Recent Sale Data	X	X
Year Built (>1992)	X	X
Estimated Stories	Only Cameron Parish	
Estimated Residential Units	Only St. Mary, St. James, St. Charles, and Plaquemines parishes	
Bedrooms	Only Cameron, Assumption, and St. James parishes	
Foundation Type	Only Cameron Parish	

Table 4 compares the relative strengths and weaknesses of each parcel dataset alongside the NSI, which are used for parcel-level information. Each data source is discussed further in the subsections

that follow.

Table 4. Comparison of Relative Potential Value of Dataset Contributions to CLARA

ATTRIBUTE	NSI (CORELOGIC, ESRI BUSINESS, HAZUS, CENSUS)	HIFLD (CORELOGIC, DUN & BRADSTREET)	ATTOM
COST	FREE VIA PRELIMINARY DATA USE AGREEMENT	FREE VIA SECURE AND LICENSED DATA AGREEMENT	REQUIRES ANNUAL SUBSCRIPTION POLYGONS AND POINTS OF INTEREST ARE A SEPARATE PRODUCT
COVERAGE	NO QUALITY OR COMPARATIVE STATISTICS	JEFFERSON DAVIS PARISH MISSING FROM CORELOGIC NO QUALITY OR COMPARATIVE STATISTICS	
SPATIAL ACCURACY	CENSUS DATA FOR SOCIAL VULNERABILITY CRITERIA AT NEAR-PARISH SCALE CORELOGIC TYPICALLY PLACES CENTROID ON STRUCTURE, WHEREAS ESRI ASSIGNED TO STREET ADDRESS	PARCELS NOT SUBDIVIDED INTO TAX LOTS	PARCELS NOT CONSOLIDATED BY OWNERSHIP ENTITY POINTS ARE CENTROIDS OF PARCELS RATHER THAN STRUCTURE
DATA ACCURACY	NEED TO VERIFY ACCURACY OF FOUNDATION TYPES YEAR BUILT HIGHLY PARISH DEPENDENT INTERFACE BETWEEN CORELOGIC AND ESRI DATA PROVIDES UNIQUE CHALLENGES FOR HOTEL POPULATIONS	RESIDENTIAL AND COMMERCIAL SPLIT REQUIRES SOME CORRECTIONS NON-RESIDENTIAL DATA NOT AS ROBUST	COMMERCIAL PROPERTY DESCRIPTIONS ARE VERY BROAD
CLEANING REQUIREMENTS	ESTIMATED FIELDS (E.G., STORIES=289, VEHICLES=$108M) INCLUDE CLEAR ERRORS ALREADY CROSS-MAPPED TO CENSUS, DAMAGE, AND NFIP DATA - BUT THIS MAY INTRODUCE SPATIAL ERRORS		REQUEST REMOVAL OF PERSONALLY IDENTIFIABLE INFORMATION FILTER OUT SOME WETLAND, WASTE, AND VACANT PARCELS (AS MAY CONTAIN STRUCTURES)

USACE NATIONAL STRUCTURE INVENTORY

In December 2019, the team obtained a review copy (subject to validation and licensing) of the latest version of USACE NSI. The NSI is a point-based structure inventory of mixed quality and coverage, developed to support various federal research efforts. The May 2019 release of USACE New Orleans District's Upper Barataria study uses this version of NSI, for example, and demonstrates the value of their methodological approach.[8] Based on the initial review, it is believed that this dataset is suitable to serve as a basis from which to build a new structure-level database for CLARA analysis.

The NSI data has not previously been used outside of the federal government, and was generously made available for the 2023 Coastal Master Plan by the Louisville District of USACE. Other state agencies across the nation, however, are – or will soon be – exploring its usage as an authoritative base layer. Among other sources, the dataset draws upon CoreLogic proprietary residential parcel data, separately licensed Esri Business Analyst data, and Microsoft building footprints (Georgist, 2019). As an additional benefit, the dataset is natively paired with both structural information from FEMA HAZUS, as well as socioeconomic indicators from other sources such as the U.S. Census Bureau.

NSI applies additional structure level data from other datasets where available. Where unavailable, these data are supplemented by older or more aggregate data available through HAZUS, and/or assumptions based on the HAZUS methodology. Figure 10 shows NSI coverage in Louisiana, with points colored by key data source (note that many points overlap at this scale). Figure 11 provides a zoomed in focus on Eastern New Orleans and St. Bernard Parish. Note that CoreLogic parcel data coverage is generally good in Orleans Parish, but that this dataset relies on older HAZUS data for residential buildings across the boundary into St. Bernard Parish.

[8] The Upper Barataria Louisiana Feasibility Report was re-released in December 2020 and is available at: https://www.mvn.usace.army.mil/About/Projects/BBA-2018/studies/Upper-Barataria-Louisiana/

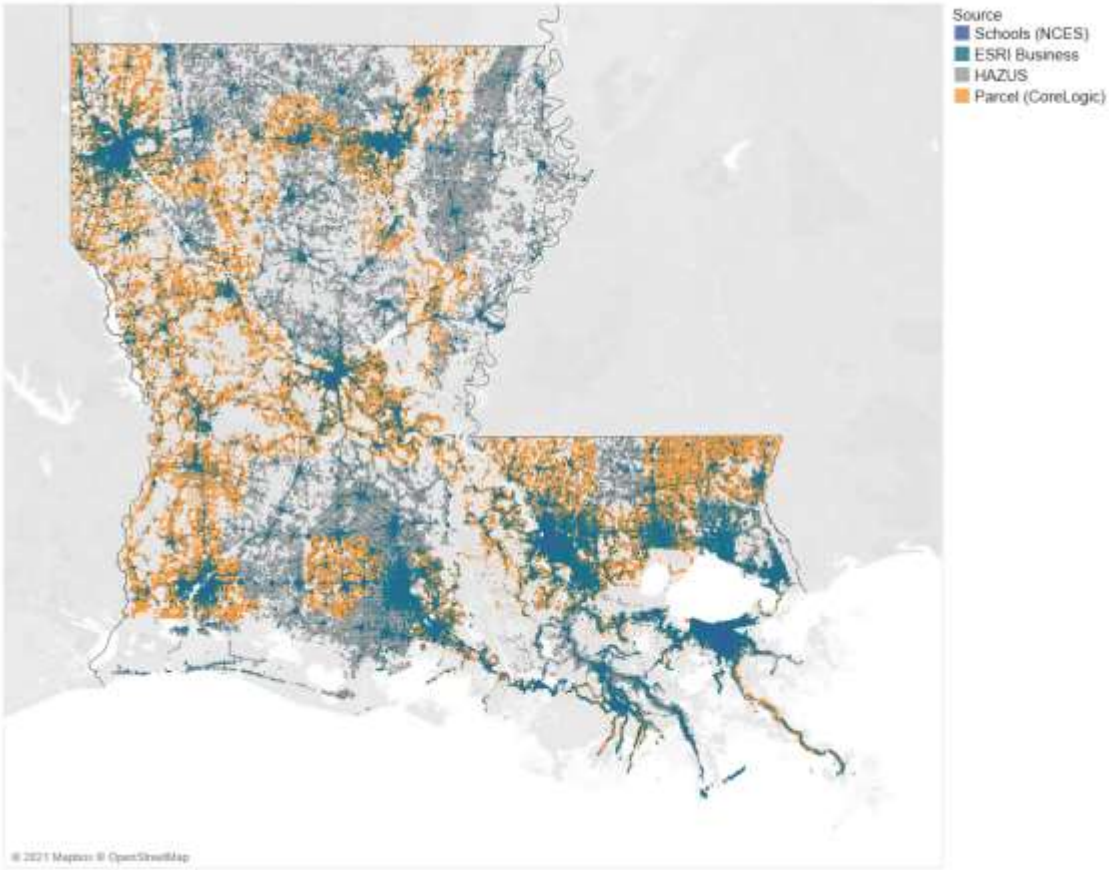

Figure 10. NSI coverage in Louisiana by data source.

Figure 11. NSI coverage: Greater New Orleans/St. Bernard example.
Note how political jurisdictions (e.g., parish boundary) determine data sources and thereby potential subsequent match quality.

By pulling data from multiple sources, NSI provides coverage of all coastal Louisiana, but there is some local/regional variation in the validity of extrapolated structural characteristics based on underlying data sources, particularly in fine-scale location (whether at the structure's centerpoint, parcel centroid, or address point along a street edge). Figure 12 provides an illustration of the implications of how NSI relates to structures versus parcels and roads by parish.

Figure 12. USACE National Structure Inventory matching methodologies near the confluence of Mississippi River and Industrial Canal.
St Claude and Lower Ninth Ward are in Orleans Parish at left, whereas Chalmette at right is in St. Bernard Parish. Orange represents where GSV and NSI structures are located within the same parcel, red where GSV and NSI structures are within 15m of each other. Because NSI structures are located along the street edge in St. Bernard Parish, the polygonal and proximity matching were unable to produce a match (in blue).

As such, the team notes that various assumptions inherent to the estimated NSI data need to be validated. For example, a March 2019 "Common Questions and Issues" document provided by USACE alongside the NSI dataset (not yet publicly available)[9] described the reliability of the included foundation height data as dependent "… on the level of decision-making and study area. The foundation types are randomly assigned to structures based on probabilities that vary by several different conditions. Users should confirm that the distribution of foundation heights is reasonable for their study area." A preliminary exploration suggested that foundation types and heights are skewed toward elevated typologies along Lake Pontchartrain, despite fewer appearing that way in GSV images. Similarly, the number of stories of a building is estimated based on several other variables, including units or employees and building footprint, rather than being directly recorded at the individual structure level. The outputs from the machine learning dataset, described in a later section, may be more reliable for these attributes in parts of the coast where these assumptions are employed by the

[9] USACE Louisville District, personal communication, December 2019.

NSI dataset.

Given the need for accurate and up-to-date data to inform the master plan's risk estimates, the NSI data was supplemented with other sources. The project team explored two other potential parcel-level data offerings: CoreLogic (some of which forms the basis of NSI) and ATTOM. Both are proprietary products that draw their data from each parish assessor's office (correcting for, but also in part accepting, the varying data quality). CoreLogic and ATTOM, however, take different approaches to their datasets, as indicated by discrepancies in their entry counts. For example, in Plaquemines Parish, ATTOM has approximately 25,136 unique geometries, versus CoreLogic's 19,437 parcels and 33,389 points.

Despite the similar breadth in coverage of the two datasets, their quality and depth of detail were compared. The following sections provide more relevant details about each of them that will be useful in deciding how to best incorporate them into risk modeling for the 2023 Coastal Master Plan.

CORELOGIC

CoreLogic data was obtained from the federal government via the Homeland Infrastructure Foundation-Level Data (HIFLD) portal. The U.S. Department of Homeland Security (DHS) has improved and diversified its offerings to State, Local, and Tribal Territories (SLTT) from what was available in 2016 as Homeland Security Infrastructure Program (HSIP) Freedom and Gold data. SLTTs with or without a Presidential Disaster Declaration (PDD) can now access open, secure, and licensed data from CoreLogic, Dun & Bradstreet, and other providers. This real estate parcel and business point data is updated quarterly and can greatly increase the spatial resolution for structure-level risk and damage calculations.[10]

The National Geospatial Agency (NGA) licenses residential and commercial parcel data from CoreLogic and releases it to the federal government as well as designated SLTT government partners. Available for download as well as geospatial web services/APIs, the data is unclassified, For Official Use Only (FOUO), and requires a need-to-know justification for HIFLD information that cannot be posted on unrestricted websites or applications. CoreLogic provides frequent update intervals (approximately 4.5 million real estate transactions per month), data quality oversight, and standardization of codes across jurisdictions. Users of CoreLogic data include real estate professionals, mortgage banks and lenders, property and casualty insurers, and 21 federal agencies. Though purchased datasets for commercial users may include Personally Identifiable Information (PII) such as ownership data, NGA has removed this for the HIFLD Secure dataset.

[10] Since downloading parcel data in November 2019, HIFLD has updated its provider to Lightbox. A brief review did not find any substantial differences since the update.

CoreLogic data is supplied in four separate files as residential or non-residential point and parcel ArcGIS File Geodatabases (in contrast to ATTOM's single point-based dataset with parcel polygons available for purchase separately). CoreLogic describes the division between these categories as:

> *...fundamentally defined by Property Indicator or a Land Use Code based on ownership and not on dwelling. For example; a record with a Property Indicator or Land Use Code that has an entry of Single Family Residence, or Mobile Home, will be delivered within the Residential Feature Class because of the ownership of the parcel or structure. In contrast to this; a record with a Property Indicator or Land Use Code of Nursing Homes or Apartment Complex, will be delivered within the Non-Residential Feature Class because of the commercial ownership of the parcel or structure.*[11]

CoreLogic also includes standardized land use codes, flags for manufactured homes, and several other construction characteristics that may or may not be used in various parishes. In the initial investigation of this dataset, it was observed that:

- The split between residential and non-residential categories is somewhat inconsistent for categories such as mobile home parks
- Non-residential assets appear to have less detailed information
- Parcels are not subdivided into tax lots
- The gross square footage values for building area are empty.

In addition, CoreLogic currently does not include Jefferson Davis Parish. Follow-up conversations indicate that the parish is in the midst of geocoding its assessor data. Similarly, there are several municipalities within Jefferson Parish that manage their own parcel datasets independent of the assessor's office and are likewise missing from the CoreLogic data (they are, however, interpolated in the ATTOM dataset). For these reasons, the team used the polygonal parcel boundaries from the CoreLogic data in the analysis, but deferred to ATTOM's value-added analysis for the database's parcel characteristics.

ATTOM DATA SOLUTIONS

For comparison, sample data of a competing product was obtained from ATTOM Data Solutions. Though the Data-as-a-Service (DaaS) licensing terms are generous, ATTOM's primary disadvantage is cost (as HIFLD Open, Secure, and Licensed data are available free-of-charge to CPRA). Specifically, the team was interested in point-based property and owner data provided in tax assessor files as well as their proprietary market valuation metrics. Separate products are available for parcel boundaries as well as points of interest (comparable to Dun & Bradstreet). Similar to CoreLogic, ATTOM has standardized numeric codes to represent tax assessor data that may vary between parishes in

[11] Source: https://gii.dhs.gov/hifld/data/secure/

Louisiana (let alone from counties across the entire country).

The project team evaluated ATTOM's "currency report" metadata for coastal Louisiana parishes. All jurisdictions had assessor data as of 2018 with valuation dates of May 2019, though Plaquemines (73%), St. Bernard (78%), and St. Martin (81%) parishes did have tax coverage amount relative to population statistics that fell below 90%. Most other parishes had nearly 100% coverage, though Orleans Parish was on the cusp with 90% coverage. Geocoding had less than approximately 2% unavailability in all but the following parishes (Table 5), which without further investigation may be of concern.

Table 5. ATTOM reported geocoding unavailability percentages greater than approximately 2%

Parish	Geocoding Unavailability
Vermilion	45.7%
Tangipahoa	39.5%
Lafourche	30.3%
Iberia	28.7%
Livingston	25.4%
Ascension	22.1%
St. Charles	17.3%
Jefferson	14.8%
Orleans	7.3%
St. Bernard	5.8%

Using Plaquemines Parish as an example for its range of built conditions across a large spatial area (Figure 13), property-use descriptions and building areas were mapped from ATTOM. Several artifacts were found in the data that showed its dependency on individual assessor methodologies. For example:

- Nearly all parcels were updated in 2018, with only 800 parcels updated in 2017 or earlier. The oldest entry was from 2013.
- Year of construction (rather than substantial renovation) data only applies from approximately 1992 onward. A select number of older construction dates were likely

added manually.

- Nearly 4,000 parcels had zero built area. Some of these appear to be raised buildings from aerial photographs, while others appear to be manufactured homes. Approximately 5,000 parcels contain less than 1,000 square foot buildings. Some of these buildings have areas as small as 200 square feet, which could indicate manufactured homes, though they may be self-reported or an algorithmic error. (Note: CoreLogic data does not include building area, so the team was unable to corroborate.)

ATTOM's standardized property-use classifications were typically quite broad, such as the commercial (general) category including refineries, airports, and nursing homes. In addition, there were a few outliers in classification – for example, parcels in depopulated bayous or miscategorizations of some assets (e.g., a sewage treatment plant as a mobile home). Some of these errors were to be expected given the parishes' original data quality and ATTOM's proprietary interpolation algorithms – and this reinforced the value of blending multiple data sources and conducting manual quality control.

Figure 13. Plaquemines Parish parcels categorized by ATTOM property descriptions and building areas (both residential and non-residential).

CORELOGIC AND ATTOM SUMMARY COMPARISON

In addition to the key points listed above (Table 3), a major difference between the data providers is that CoreLogic typically provides a more accurate location for individual structures than ATTOM because the latter has not consolidated contiguous parcels and relies on centroids. Furthermore, CoreLogic typically would require less data cleaning on the actual land uses.

Despite these substantial advantages of CoreLogic, there are some drawbacks. As shown in Figure 14, for example, CoreLogic typically includes two points – one at the centroid of the parcel (CEN) and the other in the center of the structure (ACQ) – whereas ATTOM has just the former. ATTOM, on the other hand, has fewer residential/non-residential classification errors.

Figure 14. Comparison of CoreLogic and ATTOM data in the Grande Terre Estates subdivision of Belle Chase, Plaquemines Parish.

Ultimately, having greater coverage of parcels beyond what is provided by the assessor office alone, more specific and corrected property use descriptions, as well as estimated market values justified the purchase of access to ATTOM data. Upon receipt from the provider, the team removed Personally Identifiable Information; processed delimitation, null data, and spacing issues; and extracted only the

required data fields across the 24 coastal parishes.

3.3 MERGING STRUCTURE- WITH PARCEL-LEVEL DATA

The team used the 780,715 Microsoft building footprints with interpolated GSV characteristics as the baseline structure dataset. The team then appended 32,277 Open Street Map structures – primarily located within Orleans Parish – for a total dataset of 812,992 structures, each with a unique CLARA ID at the end of the following process.

The first step of matching parcel-level attributes was a spatial join with polygonal parcel boundaries. CoreLogic provided 1,371,815 parcels, to which the team supplemented another 42,570 parcels in the Gretna and Kenner municipalities of Jefferson Parish (obtained from their administrators). MS/GSV structures that did not spatial join (null) were retained for subsequent address- and proximity-based matching. MS/GSV structures that spatially joined to multiple parcels (for example, a building where multiple parcels stack over the same XY points indicating vertically separated condominium-style ownership) were similarly retained for subsequent address and proximity-based matching (multi-matches).

These polygons were then used to spatially join the CoreLogic parcel to ATTOM, NSI, and DNB point data. Like the step above, null and multi-matches were retained for subsequent address- and proximity-based analysis (except NSI, which lacks addresses).

After systematizing the ATTOM and DNB address data (capitalization, highway abbreviations, etc.) the team used a hard (exact one-to-one relationship) text address comparison to identify additional matches.[12] As a last step, all null and multi-match address matches were then proximity matched to ATTOM, NSI, and DNB using a 15 m search radius (based on typical urban street width as well as traditional long lot dimensions), assigning the closest point within that distance. It was assumed that after polygonal area, alphanumeric address, and radial distance proximity matches, the team was unlikely to characterize parcel-based attributes with any level of certainty to the structures, so this was the extent of the merging process.

As a part of the QA/QC process, a data quality score was developed that examined the pairing methodology, cumulative presence of attribute fields, and overall rank for specificity of information for assigning depth damage function curves. The data pairing methodology was ranked using the

[12] The team did not check for misspelling, misnumbering, or other data entry issues, but instead relied on other matching processes in cases where address errors might have carried through.

following point-based system:

- CoreLogic Parcel Match (3)
- Exact Address Match (2) - only possible for DNB and ATTOM
- 15 m Proximity Match (1)
- GSV only (0).

The team then cumulatively scored by non-null use or occupancy type data presence:

- 3 points for all DNB (NAICS6), ATTOM (PropertyUseStandardized), and NSI (occtype)
- 2 points for two
- 1 point for one
- 0 for GSV only (or if an OSM structure that then later matched through parcel or proximity).

Last, the team ranked the data quality for assigning a depth damage function curve (to be discussed in the next section):

- DNB (3)
- ATTOM (2)
- NSI (1)
- GSV interpolation (0).

Given the potential combinations, a score of six and above is high quality data (requires more than one data source). Scores between three and five are mid/usable quality data – indicating at least a proximity match of some sort. Two is not a possible score, and zero or one indicates that the team would need to infer from available GSV data.

Figure 15 and Table 6 displays the variation in data quality across the model domain and by parish. Approximately 80% of the data is deemed high quality, with Jefferson Davis having a known issue with the lack of parcel information. Cameron and Vermilion parishes also had lower data quality, with around 50% of their data being less than high quality, and Iberville Parish had some quality issues, but fewer parcels were impacted. Overall, there do not appear to be systemic impacts beyond lacking parcel data, which was intentionally valued low in the scoring. This is most apparent in Grand Isle, Port Fourchon, and rural or bayou areas.

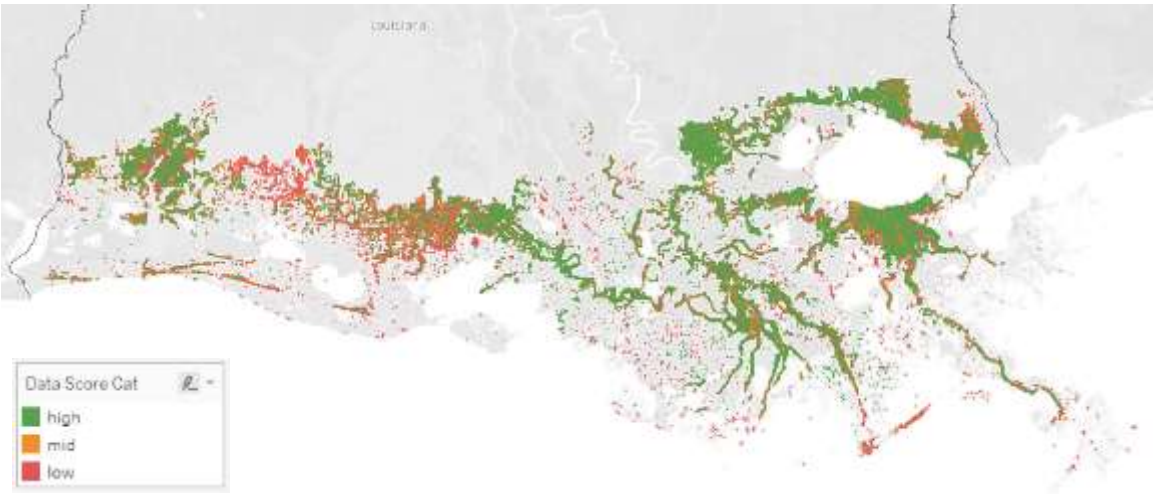

Figure 15. Data quality across the model domain.
Data quality is generally high, especially in built-up areas. The lack of reliable parcel data in Jefferson Davis Parish as well as in the bayous and along the Atchafalaya River resulted in low data scores for these areas.

Table 6. Data Score by Parish

	SCORE CATEGORY						
PARISH	**HIGH**		**MID**		**LOW**		**TOTAL**
ACADIA	1,199	76%	226	14%	159	10%	1,584
ASCENSION	41,078	91%	2,324	5%	1,590	4%	44,992
ASSUMPTION	10,231	82%	1,116	9%	1,179	9%	12,526
CALCASIEU	60,849	77%	9,125	12%	8,811	11%	78,785
CAMERON	3,193	51%	1,275	20%	1,773	28%	6,241
IBERIA	25,757	79%	3,457	11%	3,316	10%	32,530
IBERVILLE	952	60%	155	10%	480	30%	1,587
JEFFERSON	117,708	76%	26,429	17%	11,591	7%	155,728
JEFFERSON DAVIS	2	0%	3,494	38%	5,647	62%	9,143
LAFAYETTE	907	72%	213	17%	141	11%	1,261
LAFOURCHE	35,402	76%	6,092	13%	4,962	11%	46,456
LIVINGSTON	7,038	74%	1,471	15%	994	10%	9,503
ORLEANS	101,719	75%	29,389	22%	5,196	4%	136,304
PLAQUEMINES	8,205	69%	1,650	14%	2,102	18%	11,957
ST. BERNARD	15,317	87%	993	6%	1,246	7%	17,556
ST. CHARLES	17,965	80%	2,217	10%	2,241	10%	22,423

	SCORE CATEGORY						
PARISH	HIGH		MID		LOW		TOTAL
ST. JAMES	9,126	81%	1,213	11%	885	8%	11,224
ST. JOHN THE BAPTIST	16,908	87%	1,068	5%	1,495	8%	19,471
ST. MARTIN	1,260	68%	257	14%	329	18%	1,846
ST. MARY	21,974	87%	1,885	7%	1,434	6%	25,293
ST. TAMMANY	64,390	79%	10,147	13%	6,532	8%	81,069
TANGIPAHOA	7,164	90%	423	5%	371	5%	7,958
TERREBONNE	38,464	78%	7,566	15%	3,481	7%	49,511
VERMILION	12,679	45%	6,120	22%	9,245	33%	28,044
TOTAL	619,487	76%	118,305	15%	75,200	9%	812,992

3.4 CROSSWALKS AND CORRECTIONS FOR DEPTH DAMAGE CURVES

The parcel-level occupancy type, property use, and NAICS business codes allow for the team to assign depth-damage functions from HAZUS to individual structures. These were applied in that order of precedence, with NSI, ATTOM, and DNB datasets in increasing specificity. All structures have building and content damage functions, whereas some occupancy or use types also have inventory damage functions (FEMA, 2009). These were drawn from both USACE New Orleans and Galveston districts featuring common general building types to the region.

Out of 812,992 potential structures, 73,897 could not be assigned a depth-damage function using an automated approach, either due to lacking occupancy or use information or the associated description was not specific enough to determine what the structure is (e.g., a seasonal house or an oil/gas well may be located on a wetland parcel). An extreme example of generic categorization impacting potential damage calculations was the Mercedes-Benz Superdome, which was classified under miscellaneous due to its multiplicity of uses, but perhaps better characterized for this model as “COM8” (entertainment and recreation structure).

As structures with large ground square footages are likely the source of some of the largest potential damages and may have the greatest variability based on their depth-damage function, the team manually assigned occupancy types to the 1% largest in this remainder (greater than 45,749 square footage (SF)). These 619 structures were categorized alongside 13,782 other nearby structures sharing similar uses (e.g., a flagged oil tank within a larger petrochemical facility resulted in all null structures being assigned IND3) or having a systematic miscategorization (groups of manufactured homes outside of a cadastral system assigned RES2) or conflicting rental use types due to a large

ownership parcel (a medical office, COM7, within a shopping center, typically COM1). Through this quality assurance process, 1,080 centroids were identified that were not in fact structures.

The remaining 59,496 structures were then assigned generic curves based on the ground square footage of the structures. Examining the distribution of ground square footage of common structure types by occupancy or use, the team inferred thresholds of:

- Less than 1,400 SF assigned as a RES2 manufactured home (representing the median square footage, in between the dimensions of a single and double-wide; n=26,793)
- Greater than or equal to 1,400 SF and less than 4,000 SF assigned as RES1 single-family home (representing up to the 92.5th percentile of that type; n=24,897)
- Greater than or equal to 4,000 SF and less than 14,000 SF assigned as COM1 retail or restaurant establishment (representing a typical spec unit development such as a pharmacy on a half-acre pad site; n=6,297)
- Greater than or equal to 14,000 SF and less than 45,749 SF assigned randomly as COM2 (warehouse), IND2 (light industrial), or COM4 (services and utilities).

As an additional quality assurance step, the team performed a manual check on the top 0.1% of ground square footage or market value of structures by occupancy or use type to ensure any potential extreme categorization errors would not negatively impact the results. For example, in New Orleans recent land use changes at the University Medical Center New Orleans and New Orleans VA Medical Center resulted in them being mischaracterized as residential typologies. Out of the 826 centroids checked, 19 were not structures (typically large-scale AI/ML error with sunglint or river barges) and 87 were correct. The most error prone category was RES1 single family homes, of which only 18 of 580 were correct (most were in fact COM1 retail or IND2 light industrial) and their large square footage indicated that they were miscategorization outliers as opposed to indicators of systemic coding issues. There were three common explanations for these specific errors. First, some parishes had land zoned as residential that appears to have been recently redeveloped for other purposes. Second, the dominant use may be residential, especially in mixed use urban areas with attached structures, but the ground floor uses may in fact be COM1 retail or COM4 services, among other functions. Third, NSI appears to preferentially assign RES1 when the use type is unknown.

Figure 16 and Table 7 summarize the structure database by use code by both the number of centroids as well as the total ground square footage. RES1 single family homes represent 76.5% of structures as 61.3% of the ground square footage. The statistics demonstrate the importance of the quality assurance step, as RES6 nursing home and EDU1 elementary (or secondary) schools represent few of the total structures, but a large amount of ground square footage – as well as being of substantial interest for exposure and vulnerability calculations.

Figure 16. Map of asset level inventory by use type for Greater New Orleans.

Table 7. Summary of Asset Level Inventory by Use

USE TYPE	NUMBER OF STRUCTURES	PERCENT OF TOTAL STRUCTURES	TOTAL GROUND SQUARE FEET	PERCENT OF TOTAL GROUND SQUARE FEET
AGR	**3,082**	**0.4%**	**10,113,201**	**0.4%**
AGR1	3,082	0.4%	10,113,201	0.4%
COM	**50,593**	**6.2%**	**461,921,802**	**19.8%**
COM1	33,151	4.1%	276,542,896	11.9%
COM2	6,036	0.7%	71,108,087	3.1%
COM3	1,077	0.1%	9,740,994	0.4%
COM4	4,408	0.5%	50,299,595	2.2%
COM5	137	0.0%	1,168,343	0.1%
COM6	222	0.0%	8,478,744	0.4%
COM7	1,904	0.2%	13,044,640	0.6%
COM8	2,812	0.3%	24,192,733	1.0%
COM9	351	0.0%	4,138,981	0.2%
COM10	495	0.1%	3,206,789	0.1%
EDU	**1,892**	**0.2%**	**42,375,862**	**1.8%**
EDU1	1,585	0.2%	36,652,404	1.6%
EDU2	307	0.0%	5,723,458	0.2%

USE TYPE	NUMBER OF STRUCTURES	PERCENT OF TOTAL STRUCTURES	TOTAL GROUND SQUARE FEET	PERCENT OF TOTAL GROUND SQUARE FEET
GOV	**1,210**	**0.1%**	**13,469,765**	**0.6%**
GOV1	1,033	0.1%	12,084,984	0.5%
GOV2	177	0.0%	1,384,782	0.1%
IND	**12,244**	**1.5%**	**105,024,804**	**4.5%**
IND1	2,981	0.4%	11,144,982	0.5%
IND2	3,580	0.4%	43,713,257	1.9%
IND3	4,234	0.5%	30,473,539	1.3%
IND4	730	0.1%	10,876,009	0.5%
IND5	90	0.0%	3,486,586	0.1%
IND6	629	0.1%	5,330,431	0.2%
REL	**2,324**	**0.3%**	**17,483,725**	**0.8%**
REL1	2,324	0.3%	17,483,725	0.8%
RES	**740,526**	**91.2%**	**1,679,041,892**	**72.1%**
RES1	621,029	76.5%	1,427,214,555	61.3%
RES2	67,004	8.3%	90,344,203	3.9%
RES3	51,315	6.3%	148,351,556	6.4%
RES4	666	0.1%	8,085,803	0.3%
RES5	430	0.1%	3,122,641	0.1%
RES6	82	0.0%	1,923,135	0.1%
TOTAL	**811,871**	**100.0%**	**2,329,431,052**	**100.0%**
STRUCTURES REMOVED IN QA/QC	1,121	0.1%	26,388,675	1.1%

3.5 CRITICAL INFRASTRUCTURE ASSET INVENTORY UPDATES

Similar to the general structure inventory, there have been substantial improvements to data available that characterize critical infrastructure within the DHS HIFLD catalog. The team drew upon the 2017 Coastal Master Plan critical infrastructure table as well as a current Governor's Office of Homeland Security and Emergency Preparedness (GOHSEP) tracking spreadsheet to summarize previously identified strategic assets and key resources. DHS CISA now considers best practice to be a sector-based analysis (e.g., Chemical, Energy, Transportation Systems) with subsectors that map closely to HIFLD layer names (e.g., Oil and Gas Infrastructure, Aviation, Maritime Transportation Systems). Like the CoreLogic and Dun & Bradstreet data, various layers are subject to use restrictions ranging from being open to the public or secure, licensed, or FOUO.

As of this report writing, these critical infrastructure updates remain in progress, and this section will

be updated once CPRA and the Risk Assessment team have confirmed the sources and data layers to inform critical infrastructure exposure.

3.6 STRUCTURE LEVEL DAMAGE ANALYSIS IN CLARA

The new structure-level dataset presents the opportunity to estimate damage and risk at the structure level for the first time. This will improve estimates of risk, enable more targeted risk communication to residents and stakeholders, and provide more flexibility and customization when designing nonstructural projects.

The team has refactored CLARA v3.0's damage model to utilize individual structural assets as the unit of analysis. Structure attributes such as foundation heights, square footage, and the number of stories are applied to produce structure-level estimates of replacement costs and to select an appropriate damage curve. Vulnerability will be estimated using the geospatial location, and associated topographic elevation, of the building. Because flood depth exceedances are calculated at the grid point level, the exceedance curve is adjusted using the difference in topographic elevation at a building's location and the median land elevation within the building's associated grid cell polygon (see Section 2.2).

Valuation of the replacement cost is still calculated using HAZUS methodology, meaning that replacement cost is predominantly estimated as the product of square footage and a replacement cost per square foot. This still represents an improvement, given that the team will use the actual building square footage rather than an average value for buildings of the same type. The unit costs per square foot will still come from HAZUS assumptions, however. Because the team does not capture all structure attributes relevant to value (e.g., construction quality), this implies that damage estimates should still not be reported at a structure level, but instead be aggregated to a larger spatial unit such as a community scale.

Where structure-level attributes are not available, either for particular properties or in larger regions of the coast, CLARA still uses a structure-level model. In this case, however, structure attributes are sampled from a distribution of attribute values for buildings of the same type that is empirically calculated over the census block group or tract level (depending on the number of such buildings available to estimate a distribution). For example, if a foundation height is unavailable for a particular structure (due to obstruction by fences, vegetation, etc. in GSV imagery), this uncertainty is incorporated into the risk estimates through Monte Carlo sampling and propagating the resulting sampled attributes through the damage calculations. The team developed generic default assumptions and damage curves for use in the case where a building's type cannot be determined, as described in Section 3.4.

4.0 UPDATES TO STATISTICAL METHODS

4.1 JPM-OS UPDATES

The 2017 Coastal Master Plan characterized the probability of tropical cyclone occurrence using a modified JPM-OS method adapted from Resio (2007) (Fischbach et al., 2017). Storm occurrence was modeled as a stationary Poisson process, and storm attributes consisting of landfall location, heading, central pressure deficit, radius of maximum winds, and forward velocity were modeled using a conditionally independent structure. The distributions were fitted using a subset of the historical record of storms found in the National Oceanic and Atmospheric Administration's (NOAA) North Atlantic Hurricane Database (HURDAT), specifically those storms making landfall in the study region from 1950 to 2014 with a central pressure less than or equal to 985 millibars. Landfall location was given an empirical probability mass function, discretized at each degree of longitude. Heading, radius of maximum winds, and forward velocity were treated as conditionally normally distributed. Central pressure was assumed to follow a Gumbel distribution with parameters dependent on the landfall location. The distributions were trained on the assumption of stationarity throughout the historical record, with future changes in storm frequency and average intensity treated as scenario assumptions.

Several changes were made to this methodology for the 2023 Coastal Master Plan, largely in response to new methods developed by USACE Engineer Research and Development Center (ERDC) Coastal and Hydraulics Laboratory (Nadal-Caraballo et al., unpublished). The most notable of these methodological advances is an augmented version of the HURDAT dataset in which previously unobserved values for the radius of maximum winds and central pressure deficit are imputed, and which includes all tropical cyclones in the HURDAT record making landfall within the study region. This substantially increases the size of potential training data early in the historical record and decreases the number of bootstrap iterates required to characterize the sampling uncertainty of the historical record.

Additionally, the updated methods assume a Weibull distribution for central pressure, and a lognormal distribution for radius of maximum winds instead of a normal distribution; they also use a longer period of record reaching back to 1938 rather than the 1950 start date used by CLARA. The 2023 Coastal Master Plan wholly adopts the new augmented HURDAT dataset. The team evaluated and accepted the use of the lognormal distribution for radius of maximum winds on the basis of maximizing the log-likelihood of the historical record conditionally upon the resulting estimated distribution. The team elected to continue to use a Gumbel distribution, as it is parameterized by a

scale and location parameter whereas the Weibull distribution is parameterized by a scale and shape parameter. The use of the Gumbel distribution therefore permits us to adjust the average central pressure without changing the variance – in line with the scenario assumptions regarding changes in central pressure – which is not possible with the Weibull distribution. The team's understanding is that one reason for ERDC adopting the Weibull distribution was to obtain a slightly better fit far into the tail of the distribution, consistent with their charge to estimate 10,000-year surge elevations (0.0001 annual exceedance probability (AEP)). The most extreme value generated by CLARA is the 2,000-year value (0.0005 AEP), so the extreme tail considerations are less critical. Further, USACE operating guidance recommends that either one of the distributions may be used (USACE, 2012).

The team evaluated the use of 1938 as a start date for the period of record but retained the use of 1950 due to concerns about the impact of non-stationarity in the distribution of central pressure deficits. The further back the period of record goes, the less strongly climate and meteorological conditions at the beginning of the period reflect existing conditions. To further allay these concerns, the team incorporated a linear drift term into the model of historical central pressure deficit, used to estimate the distribution of central pressure deficit: this change improved the log-likelihood of the distributional fit. While Nadal-Caraballo et al. (unpublished) introduces a number of other methodological advancements, these were found to be incompatible with CLARA's risk estimation framework and were therefore not incorporated into the 2023 Coastal Master Plan. Therefore, the final joint probability function fit to the new version of CLARA is the following:

$$\Lambda(c_p, r, v_f, \theta_l, x) = \Lambda_1 \cdot \Lambda_2 \cdot \Lambda_3 \cdot \Lambda_4 \cdot \Lambda_5$$

$$\Lambda_1 = f(c_p|x) = \frac{\partial}{\partial x}\left\{\exp\left\{-\exp\left[-\frac{c_p - (a_0(x) + a_1(x)t)}{a_2(x)}\right]\right\}\right\}$$

$$\Lambda_2 = f(r|c_p) = \frac{1}{r\sigma(\mathrm{c_p})\sqrt{2\pi}} e^{-\frac{\left(\ln r - \bar{r}(c_p)\right)^2}{2\sigma^2(c_p)}}$$

$$\Lambda_3 = f(v_f|\theta_l) = \frac{1}{\sigma\sqrt{2\pi}} e^{-\frac{\left(\overline{v_f}(\theta_l) - v_f\right)^2}{2\sigma^2}}$$

$$\Lambda_4 = f(\theta_l|x) = \frac{1}{\sigma(x)\sqrt{2\pi}} e^{-\frac{\left(\overline{\theta_l}(x) - \theta_l\right)^2}{2\sigma^2(x)}}$$

$$\Lambda_5 = f(x) = \Phi(x)$$

Where the storm parameters are central pressure c_p in millibars (mb), radius of maximum windspeed r in nautical miles (nm), forward velocity v_f in knots (kt), location of landfall x in degrees longitude,[13] and landfall heading θ_l in radial degrees east of due north.

[13] CLARA utilizes an idealized Louisiana coastline represented by a straight line west to east at $29.5°N$, implying that landfall can be characterized only by the longitudinal location.

4.2 STORM SELECTION FOR THE 2023 COASTAL MASTER PLAN

The new set of available synthetic storms developed by ERDC consists of 645 storms that span a wider range of the possible Atlantic cyclone parameter space than the previous corpus of 446. For example, central pressures at landfall range from 1005 mb to 865 mb, representing everything from minor tropical depressions to Category 5 hurricanes considerably stronger than any ever observed in the Atlantic basin. “Master” storm tracks were developed that make landfall with headings that vary by 20 degrees. Each of these master storm tracks was then shifted east and west repeatedly by spacings of 60 km until enough tracks were generated to span the Gulf region. The resulting set of tracks is shown below in Figure 17. There are a total of 15 tracks that make landfall with a heading of due north, with other headings having a smaller number of tracks spaced over the study region. Seven or eight synthetic storms are placed on each track with different values for central pressure, radius of maximum windspeed, and forward velocity.

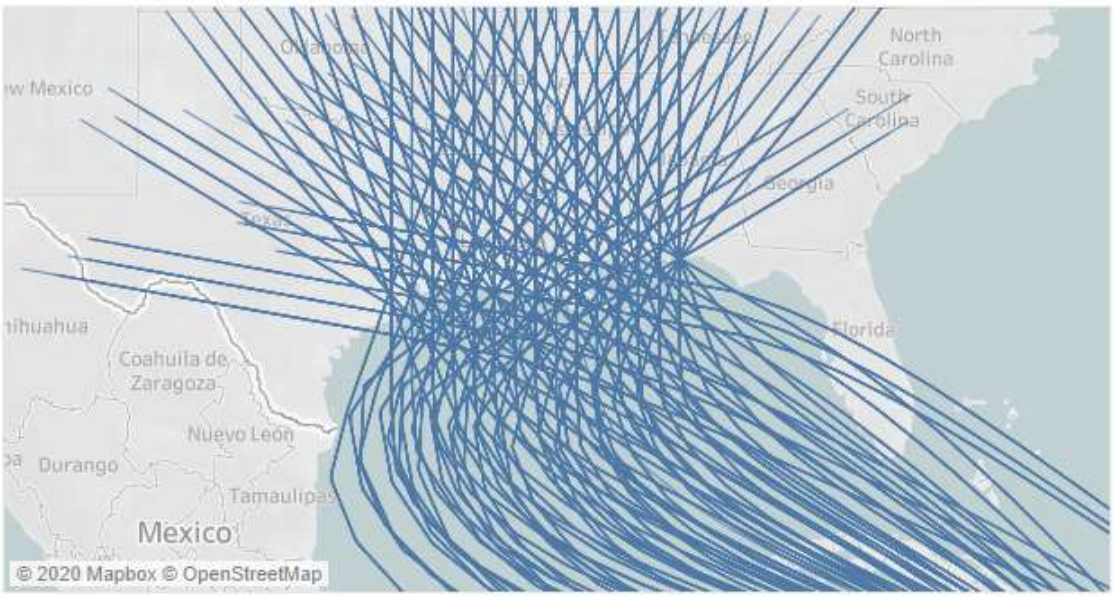

Figure 17. Synthetic storm tracks represented in the ERDC 645-storm suite.

As in previous master plans, the available corpus of synthetic storms is larger than can feasibly be simulated over the range of time periods, scenarios, and project meshes that are required to support plan development. A reduced subset of storms is needed that produces flood depth exceedance estimates similar to those which would be generated by the entire suite. Rather than analyzing a large number of reduced storm sets in CLARA, as described in Fischbach et al. (2016), the team has collaborated with ERDC to leverage their capabilities in storm set reduction.

ERDC developed a genetic algorithm that starts with a randomly selected set of storms that is small in number but sufficient for the joint marginal distributions to be identifiable. Upon requesting options for storm sets between 80 and 100 storms, ERDC produced a set of 95 storms for potential use in the 2023 Coastal Master Plan. Five of the storms were discarded from use because they do not make landfall near enough to the study region to have an appreciable impact on flood depth exceedances. Henceforth, this reduced storm set is referred to as the "90-storm set".

The team next compared estimated surge elevation exceedances based upon the remaining 90 storms from the ERDC reduced storm set to estimates derived from the full suite of 645 storms. The team then used an additional algorithm to incrementally add and remove synthetic storms for this set, five at a time, on the basis of how much the accuracy of exceedance estimates improves when compared to the reference estimates. This process is detailed in Section 4.4 below.

4.3 PRELIMINARY ANALYSIS RESULTS AND COMPARISON

ERDC's analysis was based on estimated surge elevation exceedances at 427 sample points shown in Figure 18. These points are a mix of ICM compartment centroids, unprotected CLARA grid points, and points along the boundary of enclosed protection systems. Each point was equally weighted, and the analysis examined return periods ranging from the 2-year (50% annual exceedance probability) to 10,000-year (0.0001% AEP).

Figure 18. Sample points used to evaluate reduced storm subsets.

Using CLARA, the team also ran a number of test cases for comparison, summarized as follows:

- 446 storms used by 2017 Coastal Master Plan

- 92 storms used to represent current conditions in 2017 Coastal Master Plan
- 645 storms available for use in 2023 Coastal Master Plan
- 90-storm set proposed by ERDC (surge values directly used as inputs)
- 90-storm set proposed by ERDC (surge predictions from response surface)
- 100-storm set (response surface trained on 90-storm set, with predictions on 10 additional interpolated storms)
- 321-storm set (response surface trained on 90-storm set, with predictions on 231 additional storms with extrapolated and interpolated parameters).

Sets 4 and 5 varied by whether or not the surge values used to estimate the exceedance curves were the actual ADCIRC surge values or values predicted for those storms by the CLARA response surface model. Sets 6 and 7 added more storms to the response surface's prediction set, with Set 6 including 10 storms contained in the convex hull of the 90-storm set over the parameter space. Set 7 included all storms that could be predicted when using the 90-storm set as the training set, i.e., storms excluded from Set 7 are on master tracks not represented in the 90-storm set.

For the ease of computation (and because surge and wave data at ICM compartment centroids are unavailable from 2017), the analysis focused only on sample points that represent unprotected CLARA grid points. Every case calculated surge elevation exceedances, which were then converted to surge depths using the 2023 Coastal Master Plan's existing conditions DEM; this avoids the introduction of differences from using different DEMs.

In analyzing this generated dataset, the team found that draft results from the 2023 meteorology (i.e., available synthetic storm sets) generally result in higher estimates of surge depth exceedances than results from the 2017 storm sets. This is illustrated in Figure 19, which shows the differences between the 446-storm set available in 2017 and the 645-storm set available for use in 2023. This finding is intuitive based on the wider range of storm parameters represented in the 645-storm set, including tropical depressions and tropical storms that occur more frequently.

It appeared that the ERDC 90-storm set produced sufficiently accurate estimates of flood depth exceedances for planning purposes. Table 8 summarizes the root mean squared error of the 90-storm set compared to the 645-storm baseline. Referring back to the storm selection analysis done to support the 2017 Coastal Master Plan, as described in Fischbach et al. (2016), the team found that the RMSE values shown in Table 8 are less than the RMSEs that were judged to be acceptable when selecting the 92-storm set and 60-storm set adopted in 2017 for the current and future landscapes, respectively.

Table 8. Root mean squared error (ft) over all sample points of the ERDC 90-storm set, relative to the 645-storm baseline

Return Period	Depth RMSE	Elevation RMSE
10-Year	0.44	0.79
50-Year	0.73	1.17
100-Year	0.64	1.13
500-Year	1.22	1.61

However, ERDC's 90-storm set systematically overestimated surge depth exceedances, as shown in Figure 20 over a range of return periods. The team continued to adjust the reduced storm set by adding and subtracting low-intensity storms in order to correct for this systematic bias, with the goal of identifying a storm set with a similar number of storms that exhibits similar or better RMSE with no apparent spatial patterns of bias.

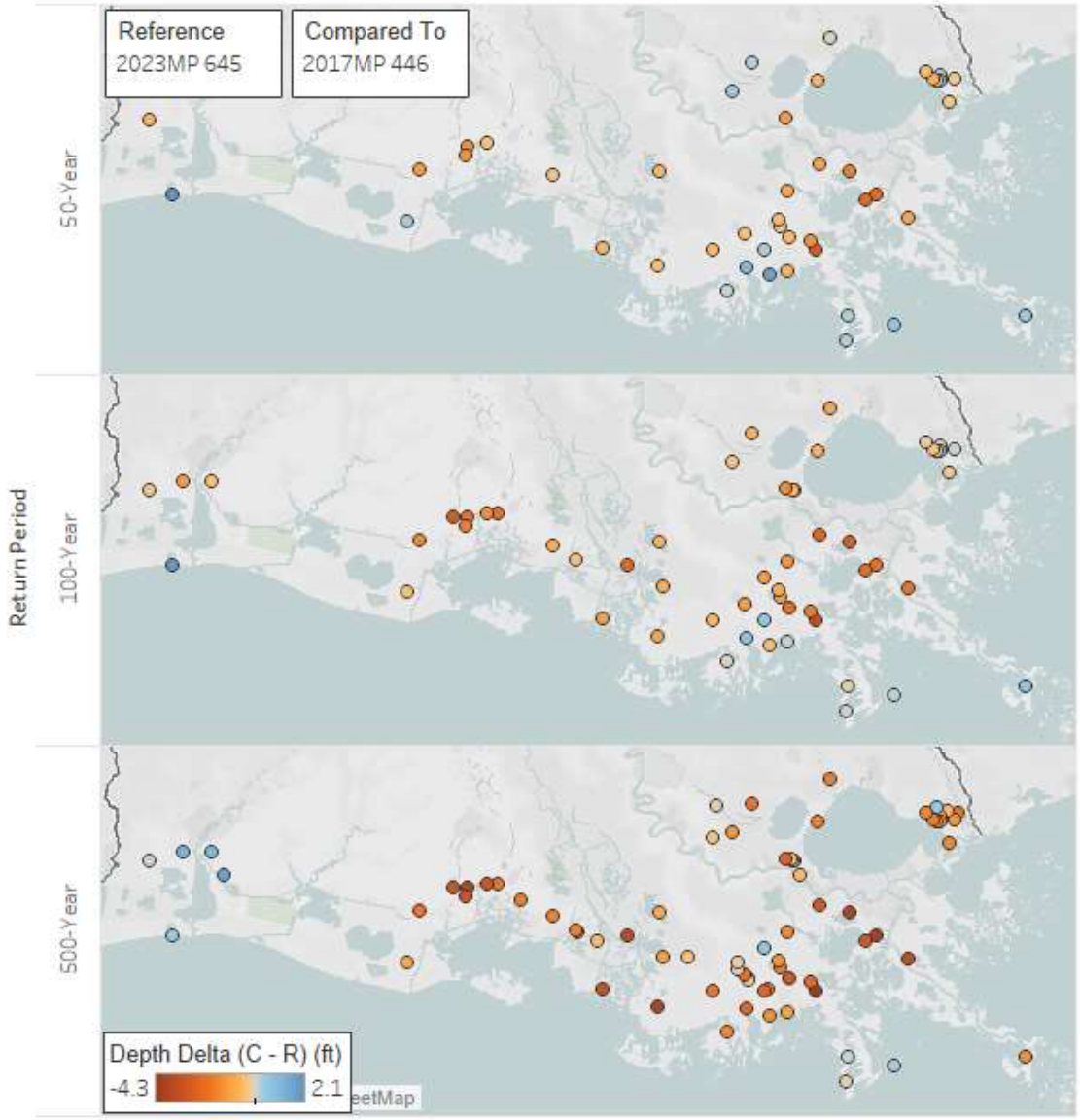

Figure 19. Differences in flood depths by return period between 645- (2023) and 446-storm (2017) sets.

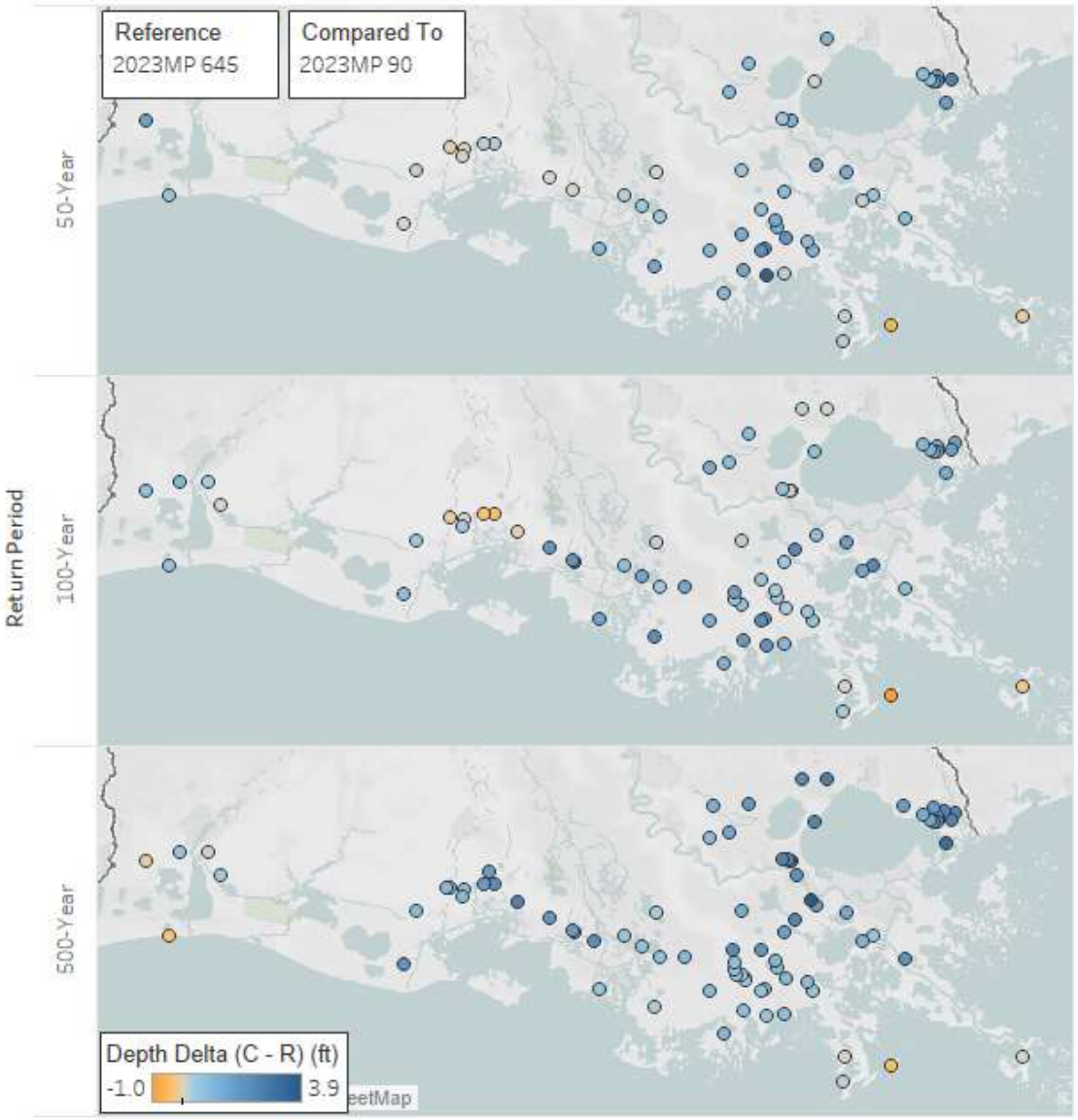

Figure 20. Differences in flood depths by return period between 645- and ERDC 90-storm sets.

4.4 FINAL REDUCED STORM SET AND ANALYSIS RESULTS

The bias identified in the ERDC 90-storm set likely stems from differences between the JPM-OS methodology used in developing the set and that which is being used for the 2023 Coastal Master Plan. The ERDC storm set reduction approach also weighted biases estimating the 10,000-year exceedance equally with the more frequent return periods relevant to the master plan. The team therefore elected to refine the ERDC 90-storm set by swapping some number of storms in and out in order to achieve better performance in light of the 2023 Coastal Master Plan JPM-OS approach. The team applied a heuristic algorithm that evaluates all possible additions to the set, selecting the addition that provides the best improvement (i.e., the largest reduction in average RMSE over the 10-, 50-, 100-, and 500-year return periods). It then evaluates all possible removals from the set, selecting the best removal. The algorithm is then said to converge at an iteration where the same storm is added and immediately removed again. While there is no guarantee that the resulting storm set is globally optimal (in the sense of being the best possible 90 storms to use), it did produce a reduced storm set which does a substantially better job of producing exceedance estimates similar to the 645-storm set.

The final set produced by the heuristic algorithm has similar characteristics to the initial 90-storm set produced by ERDC in terms of the distributions of central pressure, radius, forward velocity, landfall angle, and landfall location. However, the final set includes 38 storms not present in the ERDC set. Figure 20 and Figure 21 show the performance of the ERDC 90-storm set and the final 90-storm set respectively, as compared to the full 645-storm suite. Table 9 shows the aggregate performance as RMSE by return period over the sample points.

Table 9. Root mean squared error (ft) over all sample points of the final 90-storm set, relative to the 645-storm baseline

Return Period	Depth RMSE	Elevation RMSE
10-Year	0.03	0.11
50-Year	0.13	0.20
100-Year	0.17	0.33
500-Year	0.18	0.29

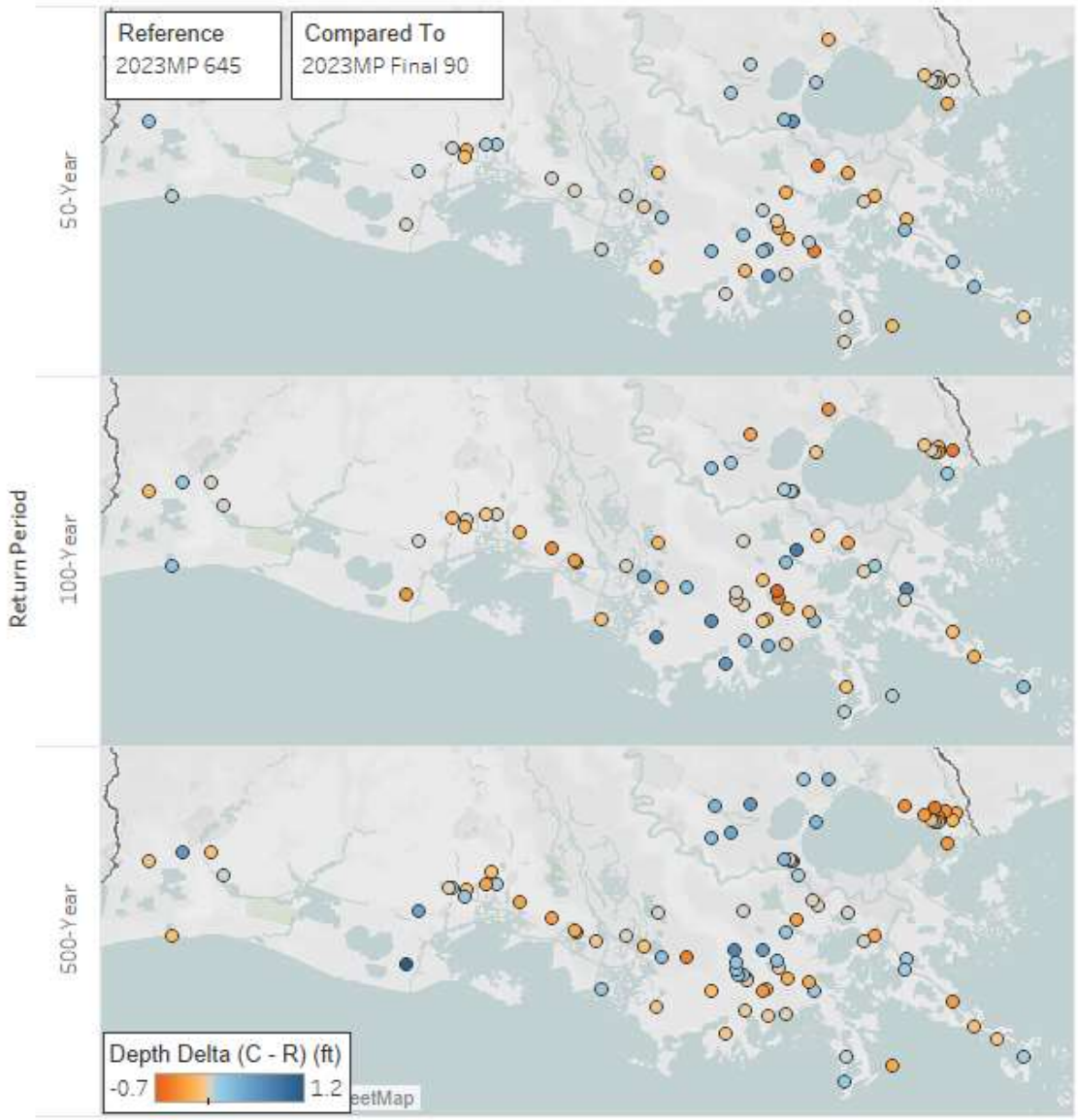

Figure 21. Differences in flood depths by return period between the 645-storm set and the final 90-storm set.

To confirm that the final 90-storm set performs well across the entire coast, the team then evaluated the differences in surge depth exceedances over all unenclosed CLARA grid points between this reduced storm set and the full 645-storm suite. The RMSE by return period, shown in Table 10, confirms that the set still performs well, with values much less than a foot at all four return periods.

Table 10. Root mean squared error (ft) over all unenclosed points of the final 90-storm set, relative to the 645-storm baseline

Return Period	RMSE
10-Year	0.28
50-Year	0.36
100-Year	0.43
500-Year	0.64

Concluding the analysis of reduced storm sets, the team provides several additional coastwide results. Figure 22 shows the surge depth exceedances from the final 90-storm set at all unenclosed CLARA grid points in Louisiana. Figure 23 shows the difference between exceedances produced by this set and the full 645-storm suite, where only differences greater than 0.5 ft are shown. In Figure 23 and Figure 24, blue indicates that the final 90-storm set values are greater than the comparison set, while orange indicates lesser values. From these comparisons, it is observed that the draft existing conditions storm surge depth exceedance values using the final 90-storm set are generally greater than those estimated for the current conditions landscape of the 2017 Coastal Master Plan. The team believes this is primarily due to the inclusion of less intense but higher-frequency storms in the 645-storm suite.

Finally, Figure 24 shows the difference between the final 90-storm set and the exceedance values produced by the 92-storm set used for current conditions in the 2017 Coastal Master Plan. The final 90-storm set also does not exhibit clear patterns of systematic bias over spatial points or across all return periods.

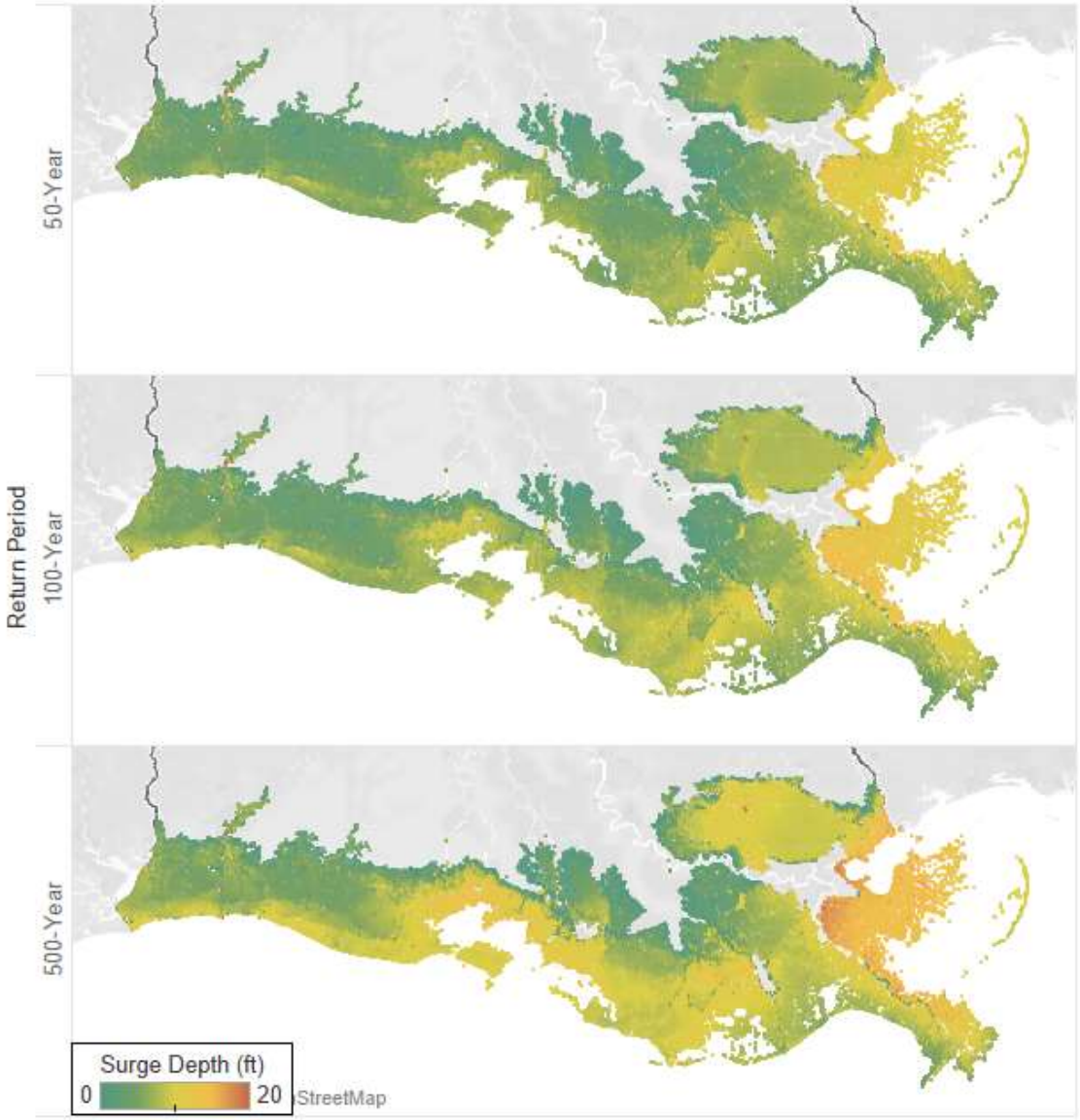

Figure 22. Surge depth exceedances associated with the final 90-storm set.

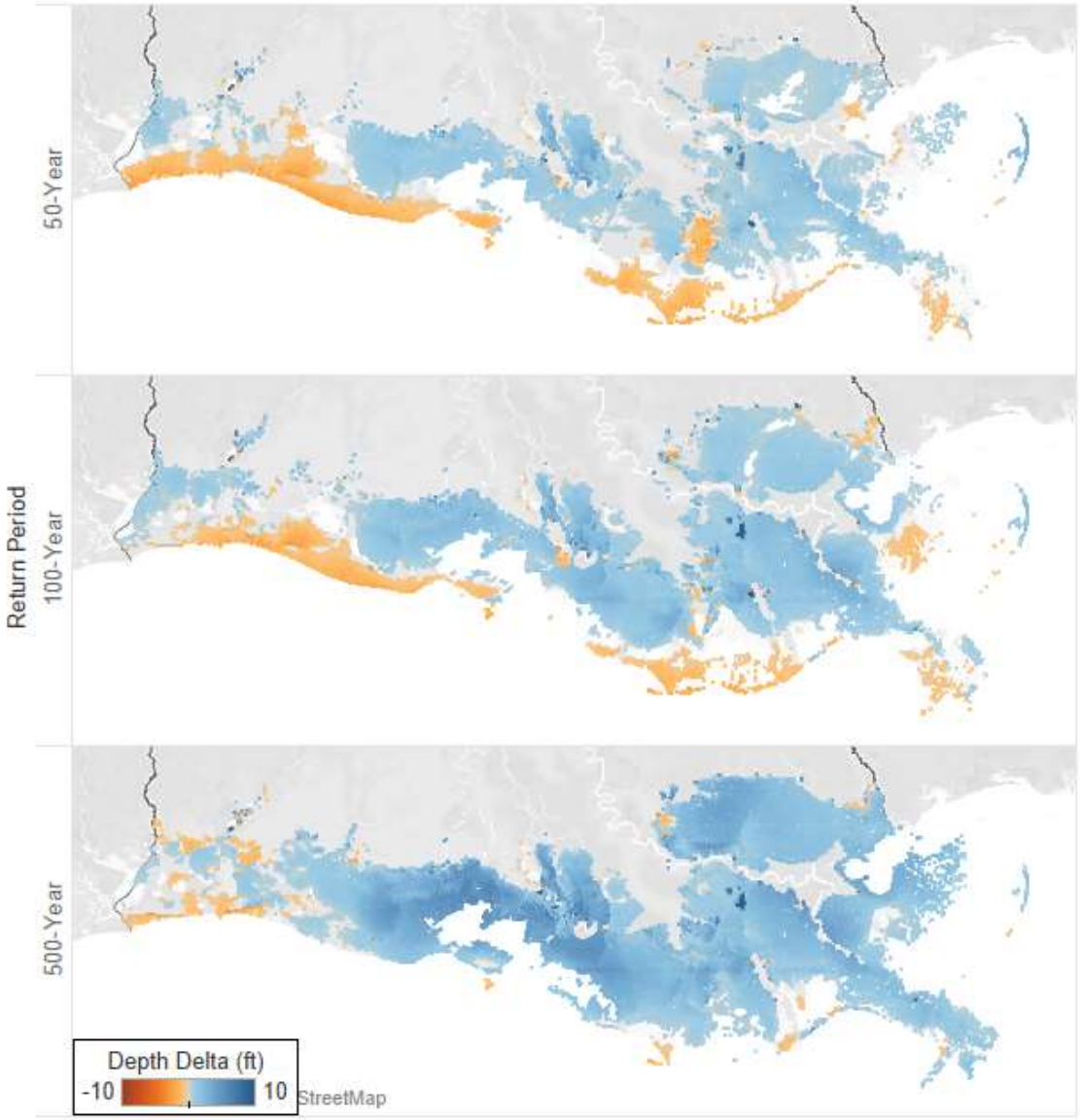

Figure 23. Difference in surge depth exceedances between the final 90-storm set and the 2017 Coastal Master Plan's current conditions case. Differences less than 0.5 ft not shown.

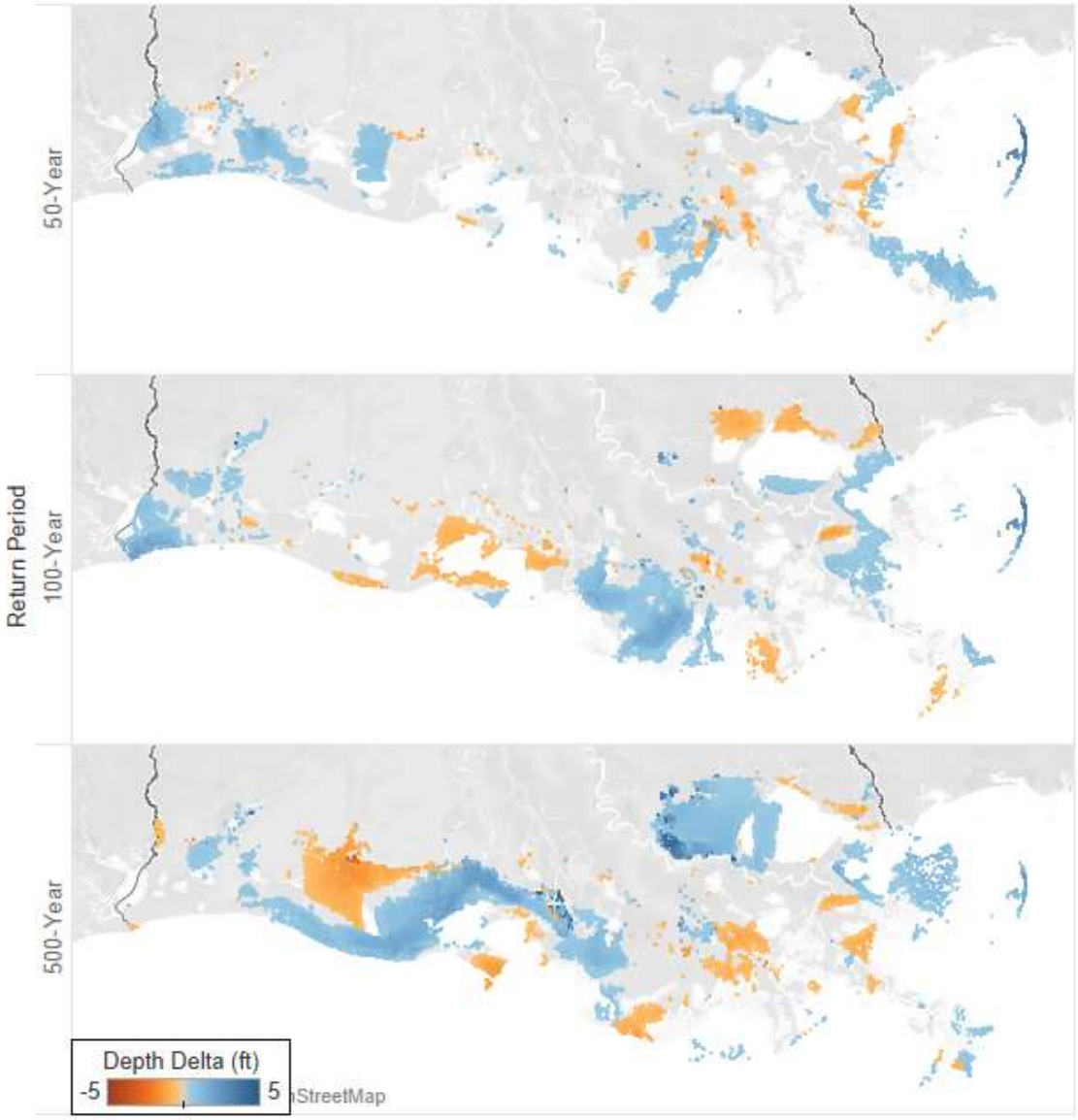

Figure 24. Difference in surge depth exceedances between the final 90-storm set and the full 645-storm suite.
Differences less than 0.5 ft not shown.

5.0 ASSET GROWTH MODEL

5.1 INTRODUCTION

Previous planning cycles have utilized multiple scenarios representing possible futures for population growth and changes in asset inventories over time. This remains a deep uncertainty about future conditions that can have a substantial impact on point estimates of baseline exposure and risk reduction achievable by the 2023 Coastal Master Plan.

The 2017 Coastal Master Plan partitioned the coastal region into three bins with different growth rates; the team parameterized future scenarios using an assumed overall coastal population growth rate and the differential in population growth between bins. The team assigned each spatial location to a bin based on a composite index of 100-year flood depth, land change, and population density. Further, population in CLARA polygons that convert entirely to open water in future conditions was assumed to be zero, meaning that residents would relocate under these circumstances and any assets would no longer be present or exposed to future flood risk.

However, risk estimate results in both the 2012 and 2017 Coastal Master Plans typically varied less across the different modeled population and asset growth scenarios than across environmental or fragility scenarios. The rank-ordering of projects during alternative formulation was thus largely insensitive to assumptions about economic growth. Given these prior findings, for 2023 Hauer (in preparation) has developed a single parameterization of future population growth.

The following subsections describe the updated methods applied for population and asset growth in CLARA v3.0 for the 2023 Coastal Master Plan, as well as opportunities to expand upon this work in future master plan iterations. The report then briefly reviews recent scientific literature regarding risk-driven mitigation that justifies the simplified approach. Finally, the team discusses implementation details and options for addressing migration induced by sea level rise for the 2023 Coastal Master Plan and notes the recommended relationship between changes in population and assets.

5.2 APPROACHES AND METHODS

POPULATION CHANGE

The growth models for previous iterations of master plan analyses were informed by a literature review

suggesting that population growth and spatial migration patterns are more conclusively driven by historic patterns and demographic factors; existing literature on risk-driven migration, as described in Section 9.2 of Fischbach et al. (2017), was as yet inconclusive. As noted above, the 2017 Coastal Master Plan employed a scenario analysis where population growth scenarios varied by the overall coastal average annual growth rate and the extent to which people disproportionately migrated to areas at lower risk.

In this section, the team outlines methods developed by Hauer and colleagues to project coastal population change, then describe show they have been adapted for the master plan and improved using the more detailed risk information produced by the CLARA model.

Hauer's contribution to the 2023 Coastal Master Plan, documented in a separate report (Hauer, in preparation), follows a similar conceptual approach to much of his previous work (Hauer et al., 2016; Hauer, 2017, 2019). Population changes over a τ-year period are calculated empirically based on historical census data, stratified by spatial units and characteristics such as population, age, sex, and race at the census block group level.[14] This yields a rate of change for each time interval. A time series model (e.g., ARIMA) is then fit to this rate-of-change data. The underlying model parameters are assumed to remain stationary moving into the future. This creates projections of population rates of change which are then translated into projected future populations.

The assumption of stationary trends in population change is a reasonable null hypothesis for baseline population projections. Future work could build off this structure to link population growth dynamics to Intergovernmental Panel on Climate Change (IPCC) Shared Socioeconomic Pathways (SSP) (O'Neill et al., 2013) via an established population normalization approach (Hauer, 2019). Hauer's projections for the 2023 Coastal Master Plan include the covariance structure between the populations of different census block groups as well as 80% confidence bounds. This permits the team to account for aleatory and epistemic uncertainty in population during the damage calculations.

POPULATION RESPONSE TO SEA LEVEL RISE

Hauer (2017) explores population migration induced by inundation due to sea level rise. This is accomplished by exploiting "migration corridors" based on IRS data on county-to-county migration (Internal Revenue Service, 2019). The method estimates a migration rate for each origin-destination pair of counties in the data, which is then normalized to forecast an expectation of where individuals displaced by inundation would relocate. Out-migrants from an affected county are assumed to leave their county and are distributed proportionally among possible destinations. If a growth model projects in-migration to a county also affected by inundation, then the growth is reduced: if *p* percent of the population of a destination county are inundated (i.e., by future tides due to sea level rise), then *p*

[14] Block groups vary in spatial extent, but typically have a population of about 600 to 3,000 people.

percent of project in-migrants are instead routed proportionally to other destinations of their respective originating counties, while *100-p* percent of the in-migrants continue to relocate to the affected destination county.

COMPATIBILITY OF HAUER'S METHODOLOGY WITH 2017 COASTAL MASTER PLAN METHODOLOGY

As mentioned above, the methods from Hauer (2017) explicitly account for land change in a binary fashion, assuming that locations are either inundated by sea level rise or unaffected by sea level rise. Any effect of population density on population growth rates which act at the census block group level or higher are captured by Hauer's modeling population growth rates at the census block group level. His previous work redistributing populations living in fully inundated areas along migration corridors expands upon assumptions made in the 2017 Coastal Master Plan in which residents of fully inundated areas are assumed to migrate out of the study domain. This approach could be adapted to incorporate land-change information from the 2023 ICM outputs, allowing the team to use ICM open-water classification to determine which areas become uninhabitable rather than using mean future tide levels under a bathtub model of sea level rise. Habitability is a relative and socially complex notion, so this may be an assumption to revisit in future master plan efforts.

The 2023 Coastal Master Plan uses methods from Hauer (in preparation) to produce a baseline population forecast, but does not utilize the migration corridor approach described above. The team has therefore retained the use of implicit prior assumptions that residents displaced by the inundation of their homes relocate to communities inland of the study region. Future master plan iterations may adopt the methodology used in Hauer (2017) to more accurately predict the migration of displaced populations. However, this method does not incorporate nonstationary endogenous feedbacks in migration dynamics, and would need to be modified to model intra-parish relocations, which could be significant in some coastal Louisiana regions with substantial variability in vulnerability within the parish (e.g., Jefferson Parish).

REVIEW OF SCIENTIFIC KNOWLEDGE OF RISK-INDUCED DEVELOPMENT AND MIGRATION

The method described above considers only stationary endogenous migration and migration due to the loss of habitable land. This therefore carries the implicit assumption that migration is not further affected by storm surge-based flood risk. The "levee effect" – the extent to which migration is influenced by risk – is an active field of study. Many researchers are attempting to quantify the strength of a levee effect and the circumstances under which it occurs. A review of recent literature suggests that the state of scientific knowledge of risk-induced development is not sufficiently advanced to provide clear guidance on modeling it. The team therefore does not recommend additional modeling activities to incorporate risk-induced migration (e.g., disproportionate growth behind levees), beyond the potential use of migration triggers described above. Some relevant work is

summarized here to illustrate the current state of scientific knowledge and ideas on this issue, which should be a useful reference when considering future applications to Louisiana's coastal planning process.

Browne et al. (2018) found that in non-coastal areas, a community's participation in the National Flood Insurance Program (NFIP) led to increased growth, as measured by the number of new housing units constructed. In coastal areas, the opposite effect was found. This difference was hypothesized to be due to the greater cost of NFIP compliance in coastal regions. The study's findings do not provide enough information to estimate the effects of induced development, but they do show that risk mitigation efforts can meaningfully impact migration patterns.

Longenecker (2019) estimated the levee effect as follows: using parcel-level data, including year of construction, changes in parcel value along several levee-protected riverine areas in protected and unprotected areas were modeled. Estimates for the value of assets at risk were made, and then an exponential model predicting the value of assets at risk as a function of the distance from the levee was fit to the data. However, the calculation of asset values and the risk assessment is not described, complicating assessment of the applicability of the results beyond the study itself. The paper finds no change in risk over time compared to what is seen in unprotected communities. Several studies suggest a plausible relationship between levels of vulnerability/protection and utility, but do not assess migration decisions. For example, Fell and Kousky (2015) find that levees increase property values. Fan and Davlasheridze (2015) suggest that individuals highly value perceived reduced flood risk.

Other research is inconclusive, and many studies addressing the issue examine the effect in developing countries or in the context of international migration. Chen et al. (2017) do not find a significant relationship between individual inundation events and migration patterns in Bangladesh; Maystadt et al. (2016) did not find an effect of riverine flooding events on long-term migration patterns in Nepal. Bylander (2016) also fails to find a robust relationship between flooding in Cambodia and the migration of residents of affected areas to Thailand. Families displaced by Cyclone Aila in 2009 reported a preference to return to their previous hometown if doing so had been economically feasible (Saha, 2017). A review of papers studying hurricane recovery found only limited impacts of hurricanes on long-term migration (Cattaneo et al., 2019). For example, Fussel et al. (2017) suggests that hurricane damage does not suppress long-term population growth, except for roughly 2% of counties with growing high-density populations.

However, Koubi et al. (2016) finds that the likelihood of migration increases with self-reported perception of risk of acute events such as flooding. Extreme precipitation in Mexico is correlated with increased international migration, but only in rural areas (Nawrotzki et al., 2015). Fussel (2015) finds that vulnerable residents of hurricane-impacted cities are the slowest and least likely to return once

temporarily displaced, suggesting that effects may vary across classes or other demographic characteristics. Curtis et al. (2015) find that migration back to areas affected by extreme storm surge flooding is much stronger than would be estimated under an assumption of stationary migration rates. Migration patterns became more urbanized and concentrated after a flood event. However, Curtis et al. (2019) find that this recovery in non-metropolitan areas is smaller and shorter-lived than in metropolitan areas, suggesting differential rates of recovery at different levels of urbanicity.

TRANSLATING POPULATION GROWTH TO ASSETS

Regardless of the modeled drivers of growth, the team also needed to consider details such as the location where new assets are assigned and their structural attributes (e.g., foundation heights, square footage). In CLARA v3.0, this uncertainty is incorporated directly into the approach to modeling parametric uncertainty. Consistent with prior analyses, it is assumed that the inventory of structural assets scales with population change as calculated at the census block group level.

However, rather than explicitly incorporating land use change, marginal development, and densification into the economic model, the team calculates the empirical distribution of structural attributes such as structure type, foundation height, square footage, and ground elevation. In future time periods, the damage model utilizes Monte Carlo simulation to assign these attributes in accordance with their distribution within each block group. Assets within each block group are distributed proportionally across that block group's grid cells, and the ground elevation of each asset is assigned by sampling from the distribution of topographic elevations within each grid cell.

CONCLUSION

In CLARA v3.0, population change does not account for migration induced by sea level rise or by high-frequency flooding, tidal events, or other risk-related factors. Populations and assets inhabiting areas projected by the ICM to convert to open water are removed from the inventories, implicitly assuming that they relocate outside of the study region. For future master plan iterations, a more sophisticated implementation of this approach may allow the team to more realistically model the migration of populations whose communities are threatened by sea level rise.

The approach adopted for the 2023 Coastal Master Plan allows more continuous variation in growth compared to the assumptions used in the 2017 Coastal Master plan, stratified by census demographics. It uses an overall growth rate consistent with historical data at the census block level, but permits future work to normalize region-wide population estimates based on commonly used population forecasts.

6.0 ADDITIONAL MODEL UPDATES

6.1 UPDATED OR ADDITIONAL RISK METRICS

The 2017 Coastal Master Plan used the change in expected annual damage (EAD), estimated for each CLARA grid point and calculated under current conditions and three future time periods (Year 10, 25, and 50), as the principal risk reduction metric for estimating project cost-effectiveness and communicating flood risk. Other metrics were also reported, such as damage recurrence at different return periods (e.g., 100-year, 500-year), but EAD reduction at Year 50 remained the key risk reduction decision metric when combined with estimated project cost.

There are several known shortcomings with this approach. First, the estimates by grid point relied on simplifying assumptions about assets within each polygon that could be improved with higher resolution data (see Section 3). Second, these results only reflect snapshots in time, and do not provide information about the timing or accrual of benefits from risk reduction investments in intervening years over the course of the 50-year time period. Relatedly, because there is no stream of benefits over time, these estimates are not supportive of formal economic benefit-cost analysis, which may be of value for either decision-making or reporting. Finally, there are known problems with relying solely on EAD or other estimates of monetized damage to assets as a measure of risk or risk reduction. Because higher value assets will tend to lead to greater EAD from flooding, other things equal, this metric can potentially bias risk reduction investments towards communities with higher wealth or income profiles. Studies have suggested a potential conflict between cost-effectiveness and equity in relation to flood risk management (Lyons-Harrison, 2017; Kind, Botzen, & Aerts, 2016), and several case studies have observed such conflict in water quality management (Khadam & Kalaurachchi, 2006; Van Der Veeren & Lorenz, 2002).

For the 2023 Coastal Master Plan, the team explored the potential to improve the estimation of EAD in different spatial areas or over time and considered additional or revised risk metrics that could help to address equity or environmental justice questions. This section describes methodological improvements for EAD implemented in the newest version of CLARA, as well as additional metrics to consider household flood exposure to better support equity analysis.

SPATIAL AGGREGATION

As noted in Section 2, CLARA has used grid cell polygons as the spatial unit of analysis when estimating risk. In previous planning cycles, the model has assumed uniform flood depth exceedance curves and asset characteristics for all economic assets located within the same grid cell polygon;

structural feature values are based on averages derived from census and other data products. Moving towards a structure-level model enables much greater flexibility in defining metrics for reporting, as damage metrics can be aggregated, weighted, or transformed in post-processing. However, due to the possibility of incomplete data on some structure-level features, the team will still require simplifying assumptions such as using average or imputed values where information is missing. Consequently, while the team believes a structure-level model will be a useful step forward, the team still plans to (i) spatially aggregate metrics to larger units of analysis and (ii) avoiding any communication of structure-level model outputs.

TEMPORAL AGGREGATION

The 2017 Coastal Master Plan experimental design utilized four time periods for each environmental scenario, representing current conditions and future Years 10, 25, and 50. Cost-effectiveness of risk reduction projects was calculated as the reduction in EAD in Year 50 relative to a future without action. Subsequent to the 2017 Coastal Master Plan, the team developed an interpolation framework for converting snapshots of risk over time to a present value over the master plan's 50-year time horizon. As described in Fischbach, Johnson, and Groves (2019):

> *To better estimate how risk changes over time, we constructed flood depth exceedance curves for every year from 2015 to 2065 by linearly interpolating the depth exceedances at each return period between the time periods explicitly modeled. We then ran the damage model on an annual basis to produce a time series of how EAD changes in response to changing flood depth distributions and changes to the value of exposed assets as the coastal population changes (also modeled using interpolation between time periods).*

Interpolating flood depth exceedances, rather than EAD or other damage metrics, allows the team to capture nonlinearities in the damage relationship to inundation depth. However, the best method of interpolation is up for debate. The paper cited above used linear interpolation on flood depth exceedances. However, the factors driving changes in risk are assumed to be a mixture of linear and nonlinear functions of time. Land subsidence and changes to hurricane frequency/intensity are assumed to change at a constant rate, but sea level rise projections are nonlinear, accelerating over the planning period. The probability of system failure is modeled as a nonlinear sigmoid curve.

Once values have been interpolated, performance over time can be summarized in various ways. Options include integrating over time (e.g., present value of EAD reduction), averaging or calculating another summary statistic (e.g., expected number of inundating flood events over 50 years), or simply providing visualization of how the metrics change over time (i.e., not aggregating). CLARA will produce time series results as inputs for use by the Planning Tool.

NEW DAMAGE METRICS

With the structure-level model, the team will be able to generate more confident estimates of the number of homes that face expected damage, or damage by return period, in excess of a given value. This allows for estimates of flood impacts that are less sensitive to the value of the asset itself or biased towards wealthier areas. The team plans to set a threshold for what constitutes "meaningful" damage, and return the number of structures which are meaningfully damaged at a given exceedance probability. This threshold could be expressed as an absolute magnitude (e.g., losses from all damage categories exceeding $1,000) or in proportion to replacement cost (e.g., structural damage exceeding 20% of replacement cost). Alternatively, such a metric could be based on exposure rather than consequences by counting the number of structures inundated to a depth of *n* feet above first-floor elevation. The team recommends having at least one such metric that is less sensitive to structure values; it is anticipated that many metrics like these would be easy to produce, so the final selection would primarily be based on CPRA's perspective on salience and effectiveness for communication.

6.2 IMPROVEMENTS MADE SINCE THE 2017 COASTAL MASTER PLAN PROCESS

In this section, the report briefly outlines some additional improvements to the CLARA modeling framework that have been developed subsequent to the 2017 Coastal Master Plan, which have not been covered in more detail in previous sections.

MODELING LEVEE/FLOODWALL FRAGILITY

The 2017 implementation of CLARA made the simplifying assumption that if a levee is breached, the breach will occur at the time of peak surge elevation. A potential breach was modeled as a Bernoulli random variable. The probability of failure *p* for a given reach segment was calculated as a function of the peak overtopping rate, the length of the segment, and an assumed scenario-dependent fragility curve. Any such breaches were assumed to be full-depth and full-width along a reach, and after the time of peak surge, overtopping was calculated assuming that the structural protection has effectively had its crest height reduced to its base. For more details on the fragility approach, see Fischbach et al. (2017).

For the 2023 Coastal Master Plan, the team implemented a new approach for modeling levee fragility adapted from Johnson et al. (in preparation), which permits breaches to occur at times other than the time of peak surge. In this new approach, a uniform random variate (from 0 to 1) is drawn for each levee segment. The probability of a breach is calculated at every time-step in the overtopping time series rather than only at the time of peak overtopping. A breach is assumed to occur if and when the

probability of a breach exceeds the uniform variate. Other than timing, the team continues to make the same assumptions about the consequences of a breach. The assumptions made regarding the timing of a breach in the proposed approach present an improvement more consistent with physical reality, although it is noted that this approach does not incorporate any knowledge of time-dependencies related to geotechnical integrity under long-duration storm events.

The 2017 version of CLARA used fragility curves that are consistent with assumptions about system fragility made by USACE in the IPET and Morganza to the Gulf studies. Because results across some fragility scenarios were very similar in the 2017 analysis and in order to reduce the size of the experimental design, the 2023 version will focus on the No Fragility and IPET Low fragility scenario from the 2017 Coastal Master Plan (Fischbach et al., 2017) as a subset of these scenarios. The No Fragility case provides an upper bound on risk reduction from structural protection projects that do not fail under load, while the IPET Low Fragility scenario can be interpreted as a representative case allowing for the possibility of structural failure.

RAINFALL MODEL UPDATE

The 2017 Coastal Master Plan implementation of CLARA utilized the IPET model of rainfall associated with synthetic tropical storm events. Gabriele Villarini has developed a spatio-temporal Gaussian process model of bias in the IPET rainfall model, permitting the creation of bias-adjusted rainfall fields (Villarini et al., under review). Work is under way to produce bias-adjusted rainfall fields for the selected storm events. Depending on the timing when these estimates become available, the team will aggregate these rainfall fields to the BHU level for use in the flood depth calculations, displacing the use of the IPET model. If they are not provided in time for use in runs for the plan, the team will use the same rainfall approach as in previous versions of the master plan.

CROSS-LANDSCAPE INTERPOLATION

Previous versions of CLARA used a statistical response surface trained on ADCIRC+SWAN data to predict peak surge and wave behavior in additional storms not run through ADCIRC+SWAN. The response surface used both storm parameters (e.g., central pressure deficit and radius of maximum wind speed at landfall) and geospatial information (e.g., distance and azimuthal angle between landfall and the point of interest) (Fischbach et al., 2017), but a separate response surface was trained for each landscape scenario. This has the potential to create a computational bottleneck, as the number of ADCIRC+SWAN simulations required scales directly with the desired number of scenarios and time periods.

CLARA's linear response surface demonstrates that linear interpolation of flood depth exceedances in unprotected areas between modeled years is an appropriate modeling approach. However, the

sigmoidal behavior of overtopping/fragility dynamics and nonlinearity of damage curves means that interior flood depth exceedances and economic risk metrics should not be interpolated linearly over time. Calculating the present value of EAD reduction over time with fidelity requires flood depth exceedances to be estimated in a greater number of time periods than are planned for storm surge modeling. In unprotected areas, the team plans to temporally interpolate surge and wave behavior storm by storm over time. For modeling risk in protected areas, this will also be done around the protection system boundary, which can then be fed into overtopping calculations. The team will then run the model at a finer time interval (i.e., every five years) to further improve the accuracy of risk estimates in enclosed protection systems over the method used by Fischbach et al. (2019).

7.0 CONCLUSION

This report described a series of advancements applied to the CLARA model to support development of the 2023 Coastal Master Plan. Improvements leverage new methodologies for flood risk estimation, new data sets providing greater fidelity for economic assets, updated meteorology, and assorted changes building on lessons learned from previous planning efforts. The report also highlights some of the analysis that informed CLARA v3.0 design choices.

Key changes included:

- Updates to the CLARA model grid, unit of analysis, and mapping capabilities
- Creation of a novel data set comprising the location and risk-relevant attributes for every structure in the coastal zone
- Implementation of advancements to joint probability modeling methodologies developed by USACE
- Selection of a new reduced storm set for use in flood risk estimation
- Development of a new population growth scenario
- Incorporation of uncertainty in population change and structural attributes into the model's parametric uncertainty framework
- Addition of risk metrics that summarize expected direct economic losses over time
- More realistic fragility modeling that accounts for the possibility of levee failures to occur during surge runup, rather than only at the time of peak surge.

Some aspects of model improvements are still ongoing and expected to continue through initial testing of the 2023 Coastal Master Plan's existing conditions landscape. The team plans to revise and update this report to reflect the final changes used in model production.

8.0 REFERENCES

Bhaduri, B., Bright, E., Coleman, P., & Urban, M. L. (2007). LandScan USA: a high-resolution geospatial and temporal modeling approach for population distribution and dynamics. GeoJournal, 69(1/2), 103-117.

Browne, M. J., Dehring, C. A., Eckles, D. L., & Lastrapes, W. D. (2018). Does National Flood Insurance Program Participation Induce Housing Development?. Journal of Risk and Insurance.

Bylander, M. (2016). Cambodian migration to Thailand: The role of environmental shocks and stress. Washington DC: World Bank.

Cattaneo, C., Beine, M., Fröhlich, C. J., Kniveton, D., Martinez-Zarzoso, I., Mastrorillo, M., ... & Schraven, B. (2019). Human migration in the era of climate change. Review of Environmental Economics and Policy, 13(2), 189-206.

Chang, H. S., & Chen, T. L. (2016). Spatial heterogeneity of local flood vulnerability indicators within flood-prone areas in Taiwan. Environmental Earth Sciences, 75(23), 1484.

Chen, F., Jahanshahi, M., Johnson, D., & Delp, E. (Under review). Deep Learning-based Building Attribute Estimation from Google Street View Images for Flood Risk Assessment Using Feature Fusion and Task Relation Encoding. Under review at IEEE Transactions on Systems, Man, and Cybernetics: Systems.

Chen, J. J., Mueller, V., Jia, Y., & Tseng, S. K. H. (2017). Validating migration responses to flooding using satellite and vital registration data. American Economic Review, 107(5), 441-45.

Curtis, K. J., Fussell, E., & DeWaard, J. (2015). Recovery migration after Hurricanes Katrina and Rita: Spatial concentration and intensification in the migration system. Demography, 52(4), 1269-1293.

Curtis, K. J., DeWaard, J., Fussell, E., & Rosenfeld, R. A. (2019). Differential Recovery Migration across the Rural–Urban Gradient: Minimal and Short-Term Population Gains for Rural Disaster-Affected Gulf Coast Counties. Rural Sociology.

Fan, Q., & Davlasheridze, M. (2016). Flood risk, flood mitigation, and location choice: evaluating the National Flood Insurance Program's Community Rating System. Risk analysis, 36(6), 1125-1147.

Federal Emergency Management Agency. (2009). Multi-Hazard Loss Estimation Methodology, Flood Model: Hazus-MH MR4 Technical Manual. Washington, D.C.

Fell, H., & Kousky, C. (2015). The value of levee protection to commercial properties. Ecological Economics, 119, 181-188.

Fischbach, J. R., Johnson, D. R., Kuhn, K., Pollard, M., Stelzner, C., Costello, R.,...,Cobell, Z. (2017). Coastal Master Plan: Appendix C3-25: Storm Surge and Risk Assessment. Louisiana's Comprehensive Master Plan for a Sustainable Coast; Final Version; Coastal Protection and Restoration Authority: Baton Rouge, LA, USA.

Fischbach, J. R., Johnson, D. R., & Groves, D. G. (2019). Flood damage reduction benefits and costs in Louisiana's 2017 Coastal Master Plan. Environmental Research Communications, 1(11), 111001.

Fussell, E. (2015). The long-term recovery of New Orleans' population after Hurricane Katrina. American Behavioral Scientist, 59(10), 1231-1245.

Fussell, E., Curran, S. R., Dunbar, M. D., Babb, M. A., Thompson, L., & Meijer-Irons, J. (2017). Weather-related hazards and population change: a study of hurricanes and tropical storms in the United States, 1980–2012. The Annals of the American Academy of Political and Social Science, 669(1), 146-167.

Georgist, H. (2019). National Structure Inventory. US Army Corps of Engineers Hydrologic Engineering Center. https://github.com/HydrologicEngineeringCenter/NSI

Groves, D, Panis, T, & Sanchez, R. (2017). Coastal Master Plan: Appendix D: Planning Tool. Louisiana's Comprehensive Master Plan for a Sustainable Coast; Final Version; Coastal Protection and Restoration Authority: Baton Rouge, LA, USA.

Gu, H., Du, S., Liao, B., Wen, J., Wang, C., Chen, R., & Chen, B. (2018). A hierarchical pattern of urban social vulnerability in Shanghai, China and its implications for risk management. Sustainable cities and society, 41, 170-179.

Hauer, M. E., Evans, J. M., & Mishra, D. R. (2016). Millions projected to be at risk from sea-level rise in the continental United States. Nature Climate Change, 6(7), 691.

Hauer, M. E. (2019). Population projections for US counties by age, sex, and race controlled to shared socioeconomic pathway. Scientific data, 6, 190005.

Hauer, M. E. (2017). Migration induced by sea-level rise could reshape the US population landscape. Nature Climate Change, 7(5), 321.

Hauer, M. E., Hardy, R. D., Mishra, D. R., & Pippin, J. S. (2019). No Landward Movement: Examining 80 years of population migration and shoreline change in Louisiana. Population and Environment, 40(4), 369-387.

Johnson, D. R., & Geldner, N. B. An Efficient Flood Risk Emulator for Levee-Enclosed Systems. (unpublished research).

Khadam, I. M., & Kaluarachchi, J. J. (2006). Trade-offs between cost minimization and equity in water quality management for agricultural watersheds. Water Resources Research, 42(10).

Kind, J., Wouter Botzen, W. J., & Aerts, J. C. (2017). Accounting for risk aversion, income distribution and social welfare in cost-benefit analysis for flood risk management. Wiley Interdisciplinary Reviews: Climate Change, 8(2), e446.

Koks, E. E., Jongman, B., Husby, T. G., & Botzen, W. J. (2015). Combining hazard, exposure and social vulnerability to provide lessons for flood risk management. Environmental Science & Policy, 47, 42-52.

Koubi, V., Spilker, G., Schaffer, L., & Bernauer, T. (2016). Environmental stressors and migration: Evidence from Vietnam. World Development, 79, 197-210.

Longenecker III, H. E. (2019). Evaluating the Effects of Induced Development on Flood Hazards and Losses in US Communities with Levees (Doctoral dissertation, University of Colorado at Boulder).

Lyons-Harrison, D. (2017). Accounting for Social Vulnerability in Flood Risk Assessment in Colombo, Sri Lanka. (Doctoral dissertation, Stichting Deltares)

Maystadt, J. F., Mueller, V., & Sebastian, A. (2016). Environmental migration and labor markets in Nepal. Journal of the Association of Environmental and Resource Economists, 3(2), 417-452.

Nawrotzki, R. J., Hunter, L. M., Runfola, D. M., & Riosmena, F. (2015). Climate change as a migration driver from rural and urban Mexico. Environmental Research Letters, 10(11), 114023.

O'Neill, B. C., Kriegler, E., Riahi, K., Ebi, K. L., Hallegatte, S., Carter, T. R., . . . van Vuuren, D. P. (2013). A new scenario framework for climate change research: the concept of shared socioeconomic

pathways. Climatic Change, 122(3), 387-400. doi:10.1007/s10584-013-0905-2

Reed, D. & Plyer, A. (2019). Toward Holistic Planning for Community Adaptation on the Louisiana Coast. Unpublished Workshop Report.

Saha, S. K. (2017). Cyclone Aila, livelihood stress, and migration: empirical evidence from coastal Bangladesh. Disasters, 41(3), 505-526.

Summers, J. K., & Smith, L. M. (2014). The role of social and intergenerational equity in making changes in human well-being sustainable. Ambio, 43(6), 718-728.

U.S. Army Corps of Engineers. (2012). Operating Guidance No. 8-12: Joint Probability – Optimal Sampling Method for Tropical Surge Frequency Analysis. Washington, D.C.: U.S. Army Corps of Engineers.

U.S. Army Corps of Engineers. (2013). Final Post Authorization Change Report: Morganza to the Gulf of Mexico, Louisiana. New Orleans, LA: Louisiana CPRA, U.S. Army Corps of Engineers, and Terrebonne Levee and Conservation District.

U.S. Army Corps of Engineers. (2014). West Shore Lake Pontchartrain Hurricane and Storm Damage Risk Reduction Study: Final Integrated Feasibility Report and Environmental Impact Statement. New Orleans, LA: U.S. Army Corps of Engineers.

U.S. Army Corps of Engineers. (2016). Southwest Coastal Louisiana: Integrated Final Feasibility Report and Environmental Impact Statement. New Orleans, LA: U.S. Army Corps of Engineers.

U.S. Census Bureau. (2019). 2019 TIGER/Line Shapefiles. Suitland, MD: U.S. Census Bureau, Geography Division. Accessed from https://www.census.gov/geographies/mapping-files/time-series/geo/tiger-line-file.html.

U.S. Internal Revenue Service. (2019). Statistics of Income Tax Stats - Migration Data. Washington, DC: U.S. Internal Revenue Service, Statistics of Income Division. Accessed from https://www.irs.gov/statistics/soi-tax-stats-migration-data, last modified 24 September, 2019.

Van der Veeren, R. J. H. M., & Lorenz, C. M. (2002). Integrated economic–ecological analysis and evaluation of management strategies on nutrient abatement in the Rhine basin. Journal of Environmental Management, 66(4), 361-376.

Villarini, G., Zhang, W., Miller, P., Grimley, L., Roberts, H., & Johnson, D.R. (under review). Probabilistic rainfall generator for tropical cyclones affecting Louisiana.